

**INDIRECT ASSESSMENT OF PORE PRESSURE
EFFECTS ON COMPRESSIVE STRENGTHS AND
ELASTICITY OF SANDSTONES**

Ronnachai Dasri

A Thesis Submitted in Partial Fulfillment of the Requirements for the

Degree of Master of Engineering in Geotechnology

Suranaree University of Technology

Academic Year 2012

การศึกษาผลกระทบแบบอ้อมของแรงดันน้ำต่อกำลังกดและความยืดหยุ่นของ
หินทราย

นายรัชชัย ดาศรี

วิทยานิพนธ์นี้เป็นส่วนหนึ่งของการศึกษาตามหลักสูตรปริญญาวิศวกรรมศาสตรมหาบัณฑิต
สาขาวิชาเทคโนโลยีธรณี
มหาวิทยาลัยเทคโนโลยีสุรนารี
ปีการศึกษา 2555

**INDIRECT ASSESSMENT OF PORE PRESSURE EFFECTS ON
COMPRESSIVE STRENGTHS AND ELASTICITY OF
SANDSTONES**

Suranaree University of Technology has approved this thesis submitted in partial fulfillment of the requirements for a Master's Degree.

Thesis Examining Committee

(Assoc. Prof. Kriangkrai Trisarn)

Chairperson

(Assoc. Prof. Dr. Kittitep Fuenkajorn)

Member (Thesis Advisor)

(Dr. Decho Phueakphum)

Member

(Prof. Dr. Sukit Limpijumnong)

Vice Rector for Academic Affairs

(Assoc. Prof. Ft. Lt. Dr. Kontorn Chamniprasart)

Dean of Institute of Engineering

รณชัย ศาสตร์ : การศึกษาผลกระทบแบบอ้อมของแรงดันน้ำต่อกำลังกดและความยืดหยุ่นของ หินทราย (INDIRECT ASSESSMENT OF PORE PRESSURE EFFECTS ON COMPRESSIVE STRENGTHS AND ELASTICITY OF SANDSTONES) อาจารย์ที่ปรึกษา : รองศาสตราจารย์ ดร.กิตติเทพ เฟื่องขจร, 55 หน้า.

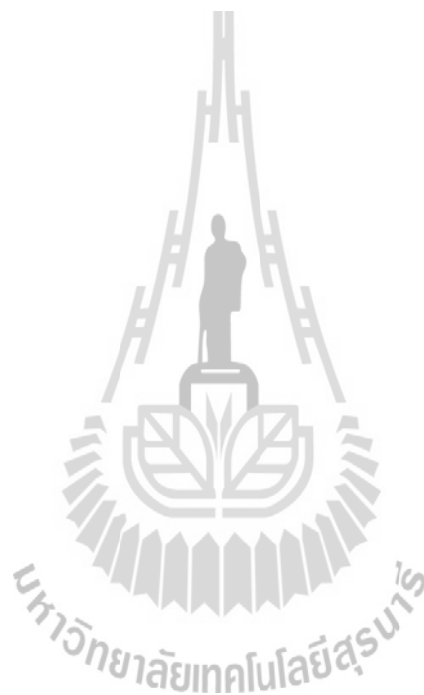
วัตถุประสงค์ของการศึกษานี้คือเพื่อศึกษาผลกระทบของแรงดันน้ำต่อกำลังกดและความยืดหยุ่นของหินทรายด้วยการทดสอบแบบผันแปรอัตราการกด การทดสอบนี้สามารถประเมินผลกระทบของแรงดันน้ำที่ขึ้นต่อคุณสมบัติทางกายภาพของหินในห้องปฏิบัติการโดยทำการทดสอบในหินทรายสามชนิดประกอบด้วยหินทรายชุดพระวิหาร ชุดภูพานและชุดภูกระดึง ซึ่งจัดเตรียมให้อยู่ในรูปสี่เหลี่ยมทรงกระบอกมีขนาด $50 \times 50 \times 100$ ลูกบาศก์มิลลิเมตร โดยหินทรายดังกล่าวมีค่าความพรุนเท่ากับ 11, 5 และ 4 เปอร์เซ็นต์ตามลำดับการทดสอบประกอบด้วย การกดในแกนเดียวและการกดในสามแกนโดยมีการควบคุมอัตราการกดให้คงที่ ความเค้นในแนวแกนที่ให้บนตัวอย่างหินจะมีอัตราการกดที่เพิ่มขึ้นคงที่ในระดับต่างกันเริ่มต้นที่ 0.001 0.01 0.1 1.0 ไปจนถึง 10 เมกะปาสคาล ต่อวินาที ความเค้นรอบข้างของตัวอย่างหินจะผันแปรจาก 0.3 7 ไปจนถึง 12 เมกะปาสคาล ซึ่งทำการทดสอบภายใต้สภาวะแห้งและสภาวะอิ่มตัวด้วยน้ำ ผลทดสอบระบุว่ากำลังกดและความยืดหยุ่นจะเพิ่มขึ้นตามอัตราการกดกำลังกดของหินที่สภาวะอิ่มตัวด้วยน้ำ มีค่าต่ำกว่าสภาวะแห้งโดยเฉพาะที่อัตราการกดและความเค้นรอบข้างที่สูง ซึ่งเป็นผลเนื่องมาจากภายใต้สภาวะดังกล่าว น้ำที่อยู่ในช่องว่างของหินจะไม่สามารถระบายออกได้ ด้วยเหตุนี้จึงทำให้เกิดแรงดันน้ำขึ้นตัวอย่างหินที่อิ่มตัวด้วยน้ำจะมีค่าอัตราส่วนปัวซองมากกว่าตัวอย่างหินแห้งเล็กน้อยเป็นผลมาจากแรงดันน้ำที่เกิดขึ้นระหว่างการทดสอบ การเพิ่มขึ้นของค่าความยืดหยุ่นของหินในสภาวะอิ่มตัวด้วยน้ำมีน้อยกว่าสภาวะแห้งซึ่งจะเห็นได้ชัดที่อัตราการให้แรงกดและความเค้นรอบข้างที่สูง

RONNACHAI DASRI : INDIRECT ASSESSMENT OF PORE PRESSURE
EFFECTS ON COMPRESSIVE STRENGTHS AND ELASTICITY OF
SANDSTONES. THESIS ADVISOR : ASSOC. PROF. KITTITEP
FUENKAJORN, Ph.D., P.E. 55 PP.

PORE PRESSURE/STRENGTH/LOADING RATE

The objective of this study is to indirectly determine the effects of pore pressures on compressive strength and elastic properties of three Thai sandstones by using variable loading rate technique. This technique is proposed here as an alternative method of determining pore pressure dependent properties of rock specimen in the laboratory. The sandstone specimens used here belong to the Phra Wihan (PW), Phu Phan (PP) and Phu Kradung (PK) formations. They are commonly found in the north and northeast of Thailand and have impacts on many engineering structures in the region. The specimens are cut and ground to obtain rectangular blocks with nominal dimensions of $50 \times 50 \times 50 \text{ mm}^3$. A polyaxial load frame has been used to apply constant confining pressures of 0, 3, 7, and 12 MPa. The applied axial stresses are controlled at constant rates of 0.001, 0.01, 0.1, 1.0 and 10 MPa/s. The specimens are prepared to test under two conditions: completely dry and fully saturated. The results indicate that the PW, PP and PK sandstones have an average porosity of 11%, 5% and 4%. For both dry and saturated conditions the compressive strengths and elastic modulus increase exponentially with the loading rate. The strengths of the saturated specimens are lower than those of the dry specimens, particularly under high confining pressures and high loading rates.

Under high loading rates and confining pressures the water cannot be drained off, and hence resulting in a built-up of pore pressure. The saturated specimens show slightly higher Poisson's ratio than do the dry specimens, probably because the pore pressure increases the specimen dilations during loading. The elastic modulus also increases with the loading rate. The dry specimens always show greater elastic modulus than do the saturated specimens. The discrepancy becomes larger under higher loading rates.



School of Geotechnology

Academic Year 2012

Student's Signature_____

Advisor's Signature_____

ACKNOWLEDGMENTS

I wish to acknowledge the funding support of Suranaree University of Technology (SUT).

I would like to express my sincere thanks to Assoc. Prof. Dr. Kittitep Fuenkajorn, thesis advisor, who gave a critical review and constant encouragement throughout the course of this research. Further appreciation is extended to Assoc. Prof. Kriangkrai Trisarn : Chairman, School of Geotechnology and Dr. Decho Phueakphum, School of Geotechnology, Suranaree University of Technology who are member of my examination committee. Grateful thanks are given to all staffs of Geomechanics Research Unit, Institute of Engineering who supported my work.

Finally, I most gratefully acknowledge my parents and friends for all their supported throughout the period of this research.

Ronnachai Dasri

TABLE OF CONTENTS

	Page
ABSTRACT (THAI).....	I
ABSTRACT (ENGLISH)	II
ACKNOWLEDGEMENTS	IV
TABLE OF CONTENTS.....	V
LIST OF TABLES.....	VII
LIST OF FIGURES	VIII
LIST OF SYMBOLS AND ABBREVIATIONS.....	XI
CHAPTER	
I INTRODUCTION	1
1.1 Background and rationale.....	1
1.2 Research objectives.....	1
1.3 Scope and Limitations	2
1.4 Research methodology	2
1.4.1 Literature review	4
1.4.2 Sample preparation.....	4
1.4.3 Laboratory testing.....	4
1.4.4 Analysis	4
1.4.5 Thesis writing.....	5
1.5 Thesis contents	5
II LITERATURE REVIEW	6
2.1 Introduction.....	6

TABLE OF CONTENTS (Continued)

	Page
2.2 Effects of pore pressure on rock	6
2.3 Conclusion of review.....	15
III SAMPLE PREPARETION	16
3.1 Introduction.....	16
3.2 Sample preparation.....	16
IV LABORATORY EXPERIMENT	19
4.1 Introduction.....	19
4.2 Rate-controlled Uniaxial compression tests	19
4.3 Rate-controlled Triaxial compression tests	20
4.4 Test results	22
V ANALYSIS	35
5.1 Introduction.....	35
5.2 Effect of pore pressure on strength	35
5.3 Effect of pore pressure on elastic properties	40
5.4 Mathematical determination.....	40
VI DISCUSSIONS CONCLUSIONS AND RECOMMENDATIONS FOR FUTURE STUDIES	44
6.1 Discussions and conclusions.....	44
6.2 Recommendations for future studies.....	45
REFERENCES	46
APPENDICES	49
APPENDIX A. DIMENSIONS AND DENSITY OF SPECIMEN.....	50
BIOGRAPHY	56

LIST OF TABLES

Table	Page
3.1 The physical properties of tested sandstones.....	17
4.1 Summary of test results of Phra Wihan sandstone.....	24
4.2 Summary of test results of Phu Phan sandstone	25
4.3 Summary of test results of Phu Kradung sandstone	26
5.1 Summary of the strength results	39
5.2 Effective stresses and pore pressures of PW, PP and PK sandstone.....	42
A.1 Dimensions and density of PW sandstone under dry condition.....	50
A.2 Dimensions and density of PP sandstone under dry condition.....	51
A.3 Dimensions and density of PK sandstone under dry condition	52
A.4 Dimensions and density of PW sandstone under saturated condition.....	53
A.5 Dimensions and density of PP sandstone under saturated condition	54
A.6 Dimensions and density of PK sandstone under saturated condition.....	55

LIST OF FIGURES

Figure	Page
1.1 Research methodology.....	3
2.1 Variation of average peak compressive strengths and corresponding standard deviations under different confining pressures.....	8
2.2 Relationships between strength as function of water content 15 of different rock types	9
2.3 Relationships between dry and saturated Young's modulus for 35 British sandstones	11
2.4 Relationships between dry and saturated uniaxial compressive strength for 35 British sandstones	13
2.5 Compressive strength of granitic rocks as a function of strain rates under the varied confining pressures	14
3.1 The rectangular blocks of sandstones with nominal size of 50 mm x 50 mm x 100 mm	17
3.2 Sandstone specimens submersed under water in vacuum chamber.....	18
4.1 A specimen for PW sandstone is tested under rate-controlled uniaxial compression	20
4.2 A polyaxial load frame used for the rate-controlled triaxial compressive strength tests.....	21

LIST OF FIGURES (Continued)

Figure	Page
4.3	Uniaxial compressive strengths testing results under loading rates varied from 0.001, 0.01, 0.1 and 1.0 MPa/s, for PW, PP and PK sandstones under dry and saturated conditions..... 27
4.4	Triaxial compressive strength testing results for PW sandstone with axial loading rates of 1, 0.1, 0.01 and 0.001 MPa/s under dry and saturated conditions..... 28
4.5	Triaxial compressive strength testing results for PP sandstone with axial loading rates of 1, 0.1, 0.01 and 0.001 MPa/s under dry and saturated conditions..... 29
4.6	Triaxial compressive strength testing results for PK sandstone with axial loading rates of 1, 0.1, 0.01 and 0.001 MPa/s under dry and saturated conditions..... 30
4.7	Elastic modulus (E) as a function of applied loading rate ($\delta\sigma_1/\delta t$) for PW, PP and PK sandstones under dry and saturated conditions..... 31
4.8	Poisson ratio (ν) as a function of applied loading rate for dry and saturated specimens..... 32
4.9	Cohesion (c) as a function of applied loading rate for dry and saturated specimens..... 33
4.10	Friction angles (ϕ) as a function of applied loading rate for dry and saturated specimens 34

LIST OF FIGURES (Continued)

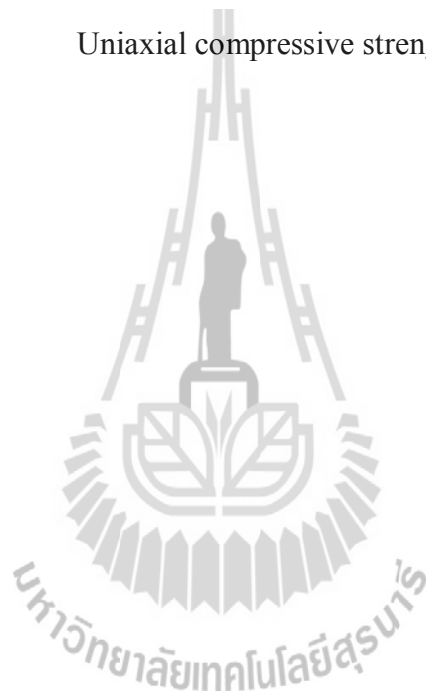
Figure	Page
5.1 Maximum principal stress (σ_1) as a function of minimum principal stress (σ_3) at failure various loading rates for dry and saturated conditions for PW sandstone.....	36
5.2 Maximum principal stress (σ_1) as a function of minimum principal stress (σ_3) at failure various loading rates for dry and saturated conditions for PP sandstone.....	37
5.3 Maximum principal stress (σ_1) as a function of minimum principal stress (σ_3) at failure various loading rates for dry and saturated conditions for PK sandstone.....	38
5.4 Pore pressures (P_w) as a function of applied loading rates ($\delta\sigma_1/\delta t$) for saturated specimens.....	43

SYMBOLS AND ABBREVIATIONS

A	=	Empirical constant for equation (4.2)
B	=	Empirical constant for equation (4.2)
c	=	Cohesion
D	=	The dry weight
E	=	Elastic modulus
n	=	The porosity
P_w	=	The pore pressure
V	=	The total bulk volume
W	=	The saturated weight
w	=	The water content
β	=	Empirical constant for equation (4.3)
κ	=	Empirical constant for equation (4.1)
ξ	=	Empirical constant for equation (4.1)
ϕ	=	Internal friction angle
α	=	Empirical constant equation (4.3)
ψ	=	Empirical constant equation (4.4)
ρ	=	The density
ν	=	Poisson's ratio
σ'_1	=	Effective maximum principal stress
σ'_3	=	Effective minimum principal stress

SYMBOLS AND ABBREVIATIONS (Continued)

σ_1	=	Maximum principal stress
σ_2	=	Intermediate principal stress
σ_3	=	Minimum principal stress
σ_u	=	Uniaxial compressive strength



CHAPTER I

INTRODUCTION

1.1 Background and rationale

Pore pressure has been known as one of the factors lowering the strength of rocks. The effect of water pressure on the intact rock strength has been observed by many researchers (Masuda, 2001; Peng and Zhang, 2007; Li et al., 2012; Sun and Hu, 1997). Several relevant tests have been conducted on various rock types to examine the effects of water pressures on rock tensile and compressive strengths. It has been found that the rock compressive strengths decrease significantly as the water content increases. The triaxial compressive strength of rocks decreases. After the adsorption of water and the yielding strength vary almost linearly with the water content. The influence of water on deformability of rocks is also reflected as a reduction of Young's modulus and increase of Poisson's ratio, which indicates that the saturated rocks will deform more than that of the dry ones under the same stress condition (Yozinaka et al., 1997; Perera et al., 2011; Li et al., 2012). The test instrumentation used to study the effects of pore water pressure usually involves triaxial pressure cells equipped with a sensitive pore measurement device. Accurate measurements of the maximum effect of the pore pressure are difficult particularly for the low porosity and low permeability rocks.

1.2 Research objectives

The objectives of this study are to determine indirectly the effects of pore pressure on compressive strength and elastic properties of three Thai sandstones. The sandstone specimens belong to the Phra Wihan, Phu Phan, and Phu Kradung formations.

The rock strength and elasticity are determined under various loading rates and confining pressures under dry and fully saturated conditions. Polyaxial load frame has been used in this study. The test frame allows a rapid loading in axial condition while the lateral confinement can be accurately maintained constant using cantilever beams.

1.3 Scope and limitations

1. Laboratory experiments are conducted on specimens from three types of sandstone prepared from Pra Wihan, Phu Kradung, and Phu Phan formations.
2. Laboratory testing made under various loading rates ranging from 0.001, 0.01, 0.1, 1 to 10 MPa/s with the confining pressures varying from 0, 3, 7 to 12 MPa.
3. Laboratory testing is performed under dry and saturated conditions.
4. Laboratory testing is performed under fully drained condition.
5. All tests are conducted under ambient temperature.
6. Up to 40 samples are tested for each rock type.
7. The nominal sizes of rectangular block are $50 \times 50 \times 100 \text{ mm}^3$.

1.4 Research methodology

As shown in Figure 1.1, the research methodology comprises 6 steps; including literature review, sample preparation, laboratory testing (uniaxial compressive strength test and triaxial test), analysis, discussions and conclusions and thesis writing.

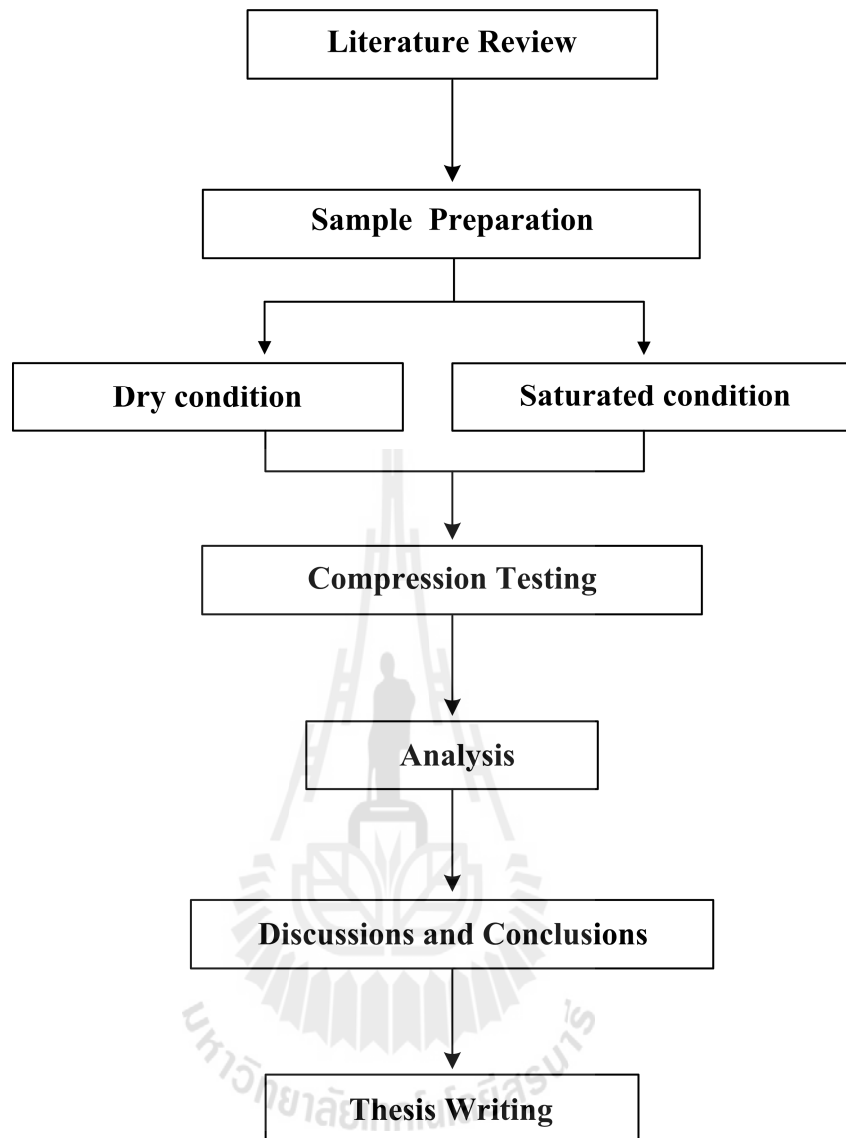


Figure 1.1 Research methodology.

1.4.1 Literature review

Literature review is carried out on experimental researches relevant to the effects of pore pressure on strengths and elasticity of rocks. The sources of information are from text books, journals, technical reports and conference papers. A summary of the literature review is given in chapter two.

1.4.2 Sample preparation

Three sandstone types are selected; Phra Wihan, Phu Phan, and Phu Kradung. Sample preparation is carried out in the laboratory at the Suranaree University of Technology. Specimens for the uniaxial and triaxial tests are prepared to obtain rectangular blocks with nominal dimensions of $50 \times 50 \times 100 \text{ mm}^3$. A minimum of 40 specimens are prepared for each rock types. Under dry condition the specimens are oven dried for 24 hours before testing. Under saturated condition the specimens are submerged under water using pressure vacuum chamber for 24 hours before testing.

1.4.3 Laboratory test

The laboratory testing is divided into two groups; uniaxial compressive strength tests and triaxial compressive strength tests. The rock strengths and elasticity are determined under various loading rates ranging from 0.001, 0.01, 0.1, 1 to 10 MPa/s with the confining pressures varying from 0, 3, 7 to 12 MPa. Three samples are tested for each loading rate and confining pressure. The sample preparation, test methods and calculation follow relevant ASTM standard practices, as much as practical. The elastic modulus and compressive strength are measured.

1.4.4 Analysis

Results from laboratory testing are analyzed to determine the effects of pore pressure on compressive strength and elasticity of three sandstones. The results from data analysis are used to comparison with other researches. The results of the three sandstones agree well with Terzaghi's effect stress law and Mohr-Coulomb criterion. This equation

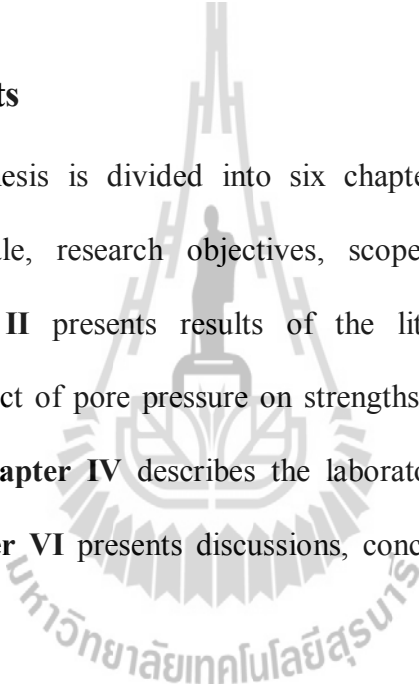
can calculate the pore pressure in saturated rock of a rock required to initiate failure from an initial state of stress defined by the maximum principal (σ_1) and the minimum principal stress (σ_3).

1.4.5 Thesis writing and presentation

All research activities, methods, and results are documented and compiled in the thesis.

1.5 Thesis contents

This research thesis is divided into six chapters. The first chapter includes background and rationale, research objectives, scope and limitations and research methodology. **Chapter II** presents results of the literature review to improve an understanding of the effect of pore pressure on strengths of rock. **Chapter III** describes sample preparation. **Chapter IV** describes the laboratory testing. **Chapter V** presents analysis method. **Chapter VI** presents discussions, conclusions and recommendation for future studies.



CHAPTER II

LITERATURE REVIEW

2.1 Introduction

Relevant topics and previous research results are reviewed to improve an understanding of the effects of pore pressure on rock. Results from the review are summarized as follows.

2.2 Effects of pore pressure on rock

Li et al. (2012) study the influence of water content and anisotropy on the strength and deformability of two sedimentary rocks by triaxial compressive tests. The water contents of both rocks are very low, for instance, 0.17% for siltstone and 0.10% for sandstone. The porosities of the tested rocks are analyzed by the technique of mercury intrusion porosimetry (MIP). It shows that the sedimentary rocks have very low porosity, 0.18% for siltstone and 0.53% for sandstone on average. The thin section analysis reveals that the siltstone contains more hydrophilic substances such as clay minerals than the sandstone, and both two sedimentary rocks are characterized by distinct beddings and laminae. Even though the water contents of two tested rocks are very low, they significantly influence the triaxial compressive strength and deformability. The reduction of strength by water content is found to be related to a reduction of friction angle in the Mohr–Coulomb failure criterion, while a reduction of m_f value in the Hoek–Brown failure criterion on the other hand. The influence of water on deformability of tested rocks is reflected as a reduction of Young's modulus and increase of Poisson's ratio, which indicates that the wet sedimentary rocks will deform more than that of the dry ones under the same stress condition. The experimental studies show that the anisotropy associated with

bedding in rock specimen plays a weakening effect on the triaxial compressive strength for both tested rocks, appearing more severely for siltstone. In general, the triaxial compression strength of rock specimens with transverse bedding planes is higher than the ones with longitudinal bedding planes no matter for siltstone or sandstone (both dry and wet conditions) under the same confining stress (Figure 2.1). With regard to the stiffness, both the tangent and secant Young's moduli of the two tested rocks with transverse bedding are less than the ones with longitudinal bedding, appearing more conspicuously for the siltstone. The paper also discusses the axial strain calibration by two different measurement techniques, one by the linear variant difference transducer (LVDT) technique and the other one by axial strain gages. It shows that the axial strain ratio coefficient k ($\epsilon_{LVDT}/\epsilon_{strain}$) decays with the deviator stress. In our present study, the secant modulus E_{strain} is usually about 1.4–1.8 times of E_{LVDT} at the peak strength point.

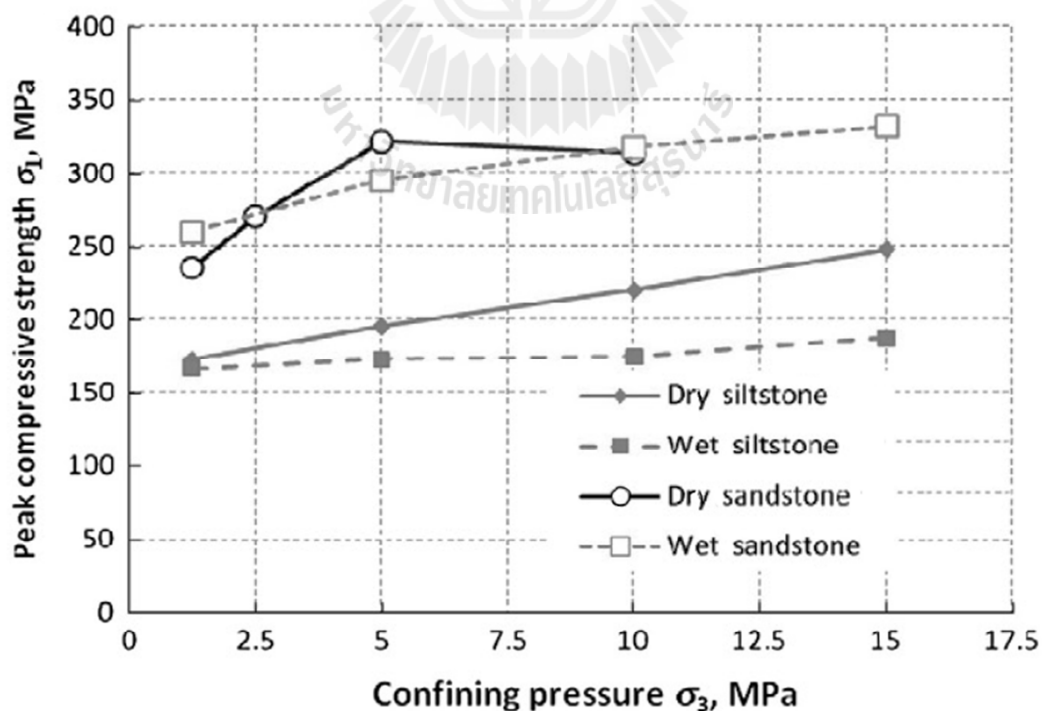


Figure 2.1 Variation of average peak compressive strengths and corresponding standard deviations under different confining pressures of dry siltstone, wet siltstone, dry sandstone and wet sandstone (Li et al., 2012).

Vasarhelyi and Van (2006) present a method for estimating the sensitivity of sandstone rocks to water content. A method for estimating the sensitivity of sandstone to its water content has been presented. From an analysis of the results of Hawkins and McConnell (1992), this sensitivity is found to be highly dependent on the effective porosity, and to be applicable to more than the strength reduction. Figure 2.2 shows the best-fit lines plotted for the 15 different rock types for water content values up to 5%. It is apparent that the strength of the rock is very sensitive to the water content an increase in water content of as little as 1% from the dry state can have a marked effect on strength. An advantage of the presented method is that less tests are necessary for calculating the influence of the water content on the rock properties. From measurements of the density and the uniaxial compressive strength in case of dry and saturated petrophysical states, the strength as a function of water content can be easily determined, both in terms of relative (i.e. water content as a percentage of the rock mass) and absolute (i.e. degree of saturation) scales. The sensitivity of other mechanical constants (i.e. Young's moduli, tensile strength, etc.) to changes in water content is likely to be similar to the sensitivity of the uniaxial compressive strength, and thus, this method could be used to estimate the water content sensitivity of these mechanical properties, as well.

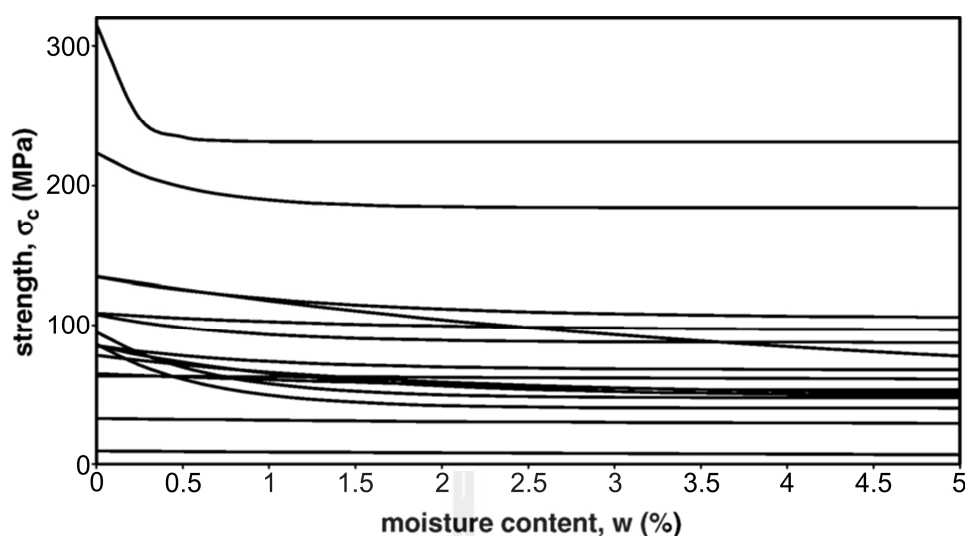


Figure 2.2 Relationships between strength (σ_c) as function of water content (w) 15 of different rock types for water content values up to 5% (Vasarhelyi and Van, 2006).

Li and Reddish (2004) present the preliminary results from laboratory based tests carried out on UK coal strata, aimed at quantifying the effects of water on rock properties, particularly on broken rocks, which are common in the subsidence overburden post mining. This approach specifically refers to the UCS, UTS and the relationship between time and water content of intact and broken rocks. Comparisons are made between these two rock conditions. The experimental results and analytic solutions show that more water can penetrate into broken rocks within shorter time. The strength of rocks can be deteriorated due to water or breaking. The water can make already broken rocks fail more easily. Also, proportionately more strength will be lost due to breaking when rocks are saturated. The state, intact or broken, appears to predominantly control the friction angle. The degree of saturation controls the cohesion. Further work is being undertaken on testing the strength of rocks at various moisture contents.

Vasarhelyi (2003) presents the unconfined compressive strength (UCS), the tangent and secant Young's modulus of 35 British sandstones are analysed statistically.

The data for UCS and tangent/secant Young's modulus given in a paper by Hawkins and McConnell (1992) have been analysed and a linear regression established between the petrophysical constants of the dry and saturated materials. Although the 35 British sandstones have different mineral contents, porosity, grain size, etc., the high R^2 values show there is a distinct relationship between the dry and saturated properties. Statistically the saturated UCS is 75.6% of the dry ($UCS_{sat} = 0.759UCS_{dry}$), while the saturated tangent and secant moduli are 76.1 and 79.0% of the dry samples respectively (Figure 2.3). The slopes of the lines are close to each other; thus it can be assumed that the influence of the degree of saturation is the same for the different petrophysical constants. The results of sandstones tested in the dry and saturated states were investigated and petrophysical constants derived. Although the sandstones have different mineral contents, grain size, porosity, etc., the results show the same general characteristics. The relationship between the different petrophysical constants is examined.

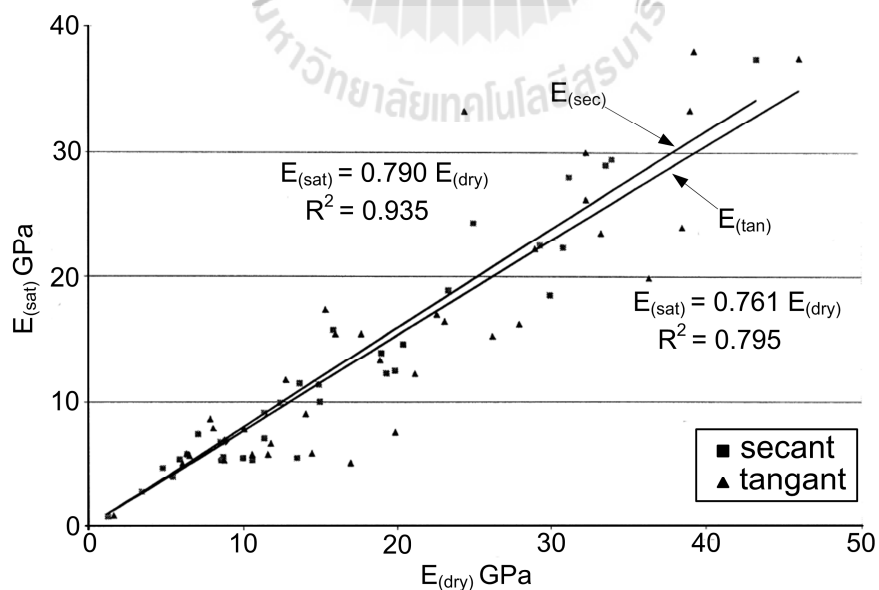


Figure 2.3 Relationships between dry and saturated Young's modulus for 35 British sandstones (Vasarhelyi, 2003).

Yozinaka et al. (1997) study the pore pressure changes and strength mobilization of soft rocks in consolidated-undrained cyclic loading triaxial tests. Changes in the pore pressure during CU (Consolidated-Undrained) cyclic loading triaxial tests on fully saturated specimens of four Miocene soft rocks, i.e. Ohya tuff, Yokohama siltstone, Kobe mudstone and sandstone are analyzed. As a result, three modes of failure, i.e. brittle, brittle-ductile and ductile can be recognized, and other characteristic stress levels e.g. crack initiation stress, plastic flow/gliding stress, dilation stress, etc. identified. The mobilization of the strength of these rocks in terms of cohesion and internal friction angle is then discussed. A procedure for the estimation of the rock cohesion strength is first introduced on the basis of the modified Griffith's failure criterion. The determination of the mobilized friction angle at any state of stress during the tests follows.

Fredrich et al. (1995) determine the induced pore pressure response, described by the Skempton ratio B , of tuff and sandstone during undrained loading. The tuff samples, from a vertical borehole, are in varying stages of devitrification and alteration to various authigenic phases, including clay, zeolite, feldspar, and quartz. Two experiments were performed on synthetic (glass) sandstones with porosities of approximately 20 and 30%. This study differs from previous work in two significant ways. First, a highly accurate transducer was designed which allowed us to explore the range in behavior up to applied confining pressures of 400 MPa. Second, we performed simultaneous measurement of axial and radial strain, thereby allowing us to correlate the induced pore pressure response with the measured bulk compressibility. Fully saturated tuff and sandstone are characterized by a B value close to one at near-zero effective pressures. For partially to fully saturated vitric and zeolitic non-welded air-fall tuffs with high matrix compressibility, B is close to one for "effective" (i.e., confining minus pore) pressures from about 25 to 50 MPa (corresponding to applied pressures of 400 MPa). For more rigid silicified zeolitic and feldspathic tuff, B is reduced to 0.7-0.8 at intermediate effective pressures of about 10-50 MPa. For the well-

in durated sandstones, B is highly pressure sensitive at low effective pressures due to the closure of low aspect ratio pores and micro cracks. At higher effective pressures, B attains an approximately constant value substantially less than one, which increases with the measured drained bulk compressibility.

Hawkins and McConnell (1992) determine the influence of the water content on the strength of 35 sandstones (Figure 2.4). They found that the relationship between water content and uniaxial compressive strength could be described by an exponential equation of the form

$$\sigma_c(w) = ae^{-bw} + c \quad (2.1)$$

where $\sigma_c(w)$ is the uniaxial compressive strength (MPa), w is the water content (%) and a , b and c are constants. It is obvious that the strength at zero water $\sigma_{c0} = a + c$, the strength at full saturation $\sigma_{csat} = c$. The parameter b is a dimension less constant defining the rate of strength loss with increasing water content.

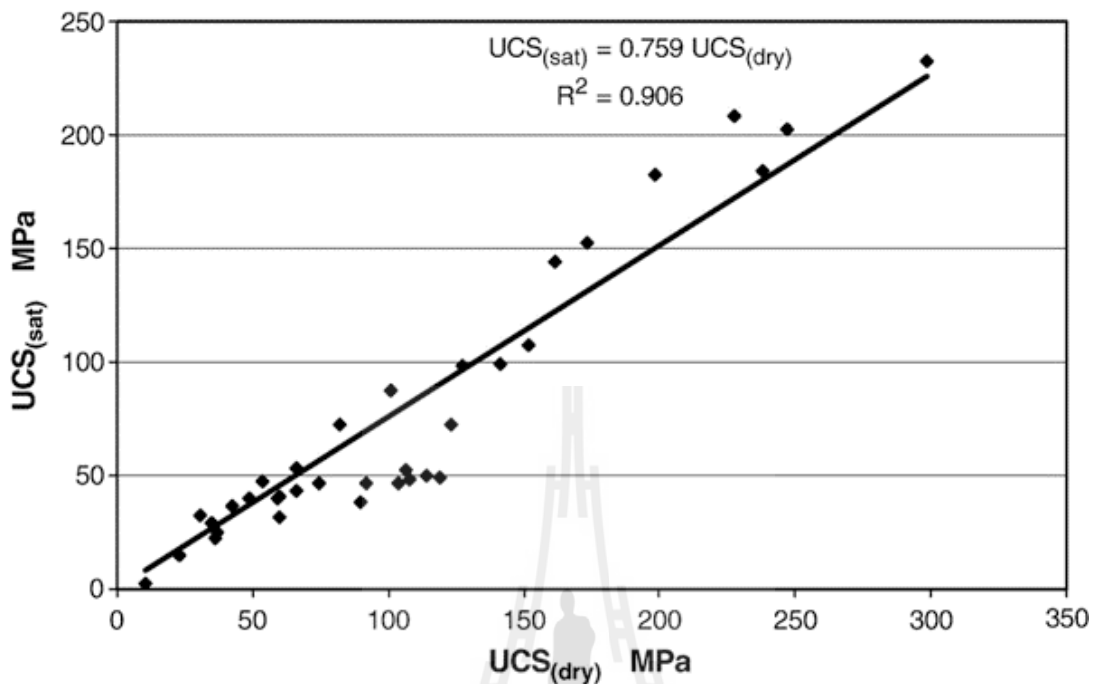


Figure 2.4 Relationships between dry and saturated uniaxial compressive strength (UCS) for 35 British sandstones (Hawkins and McConnell, 1992).

Masuda (2001) studies the effects of water on rock strength in granite and andesite. The failure strengths of granite and andesite have been measured under various conditions of strain rate and confining pressure both in the dry and wet states. Constant-stress creep tests for granitic samples have been also conducted (Figure 2.5). All specimens show that the failure strength decreased linearly as the logarithm of the strain rate decreased. The strain rate dependence of the failure strength is increased at higher confining pressures. The strain rate effect is more apparent on the failure strengths of wet samples than dry samples in lower confining pressure ranges. In the constant-stress creep experiments, the creep failure strength decreased as the logarithm of the time to failure increased. Time-dependent failure strength of all rocks observed in the regime of the present study may be interpreted by subcritical crack growth assisted by the stress corrosion mechanism.

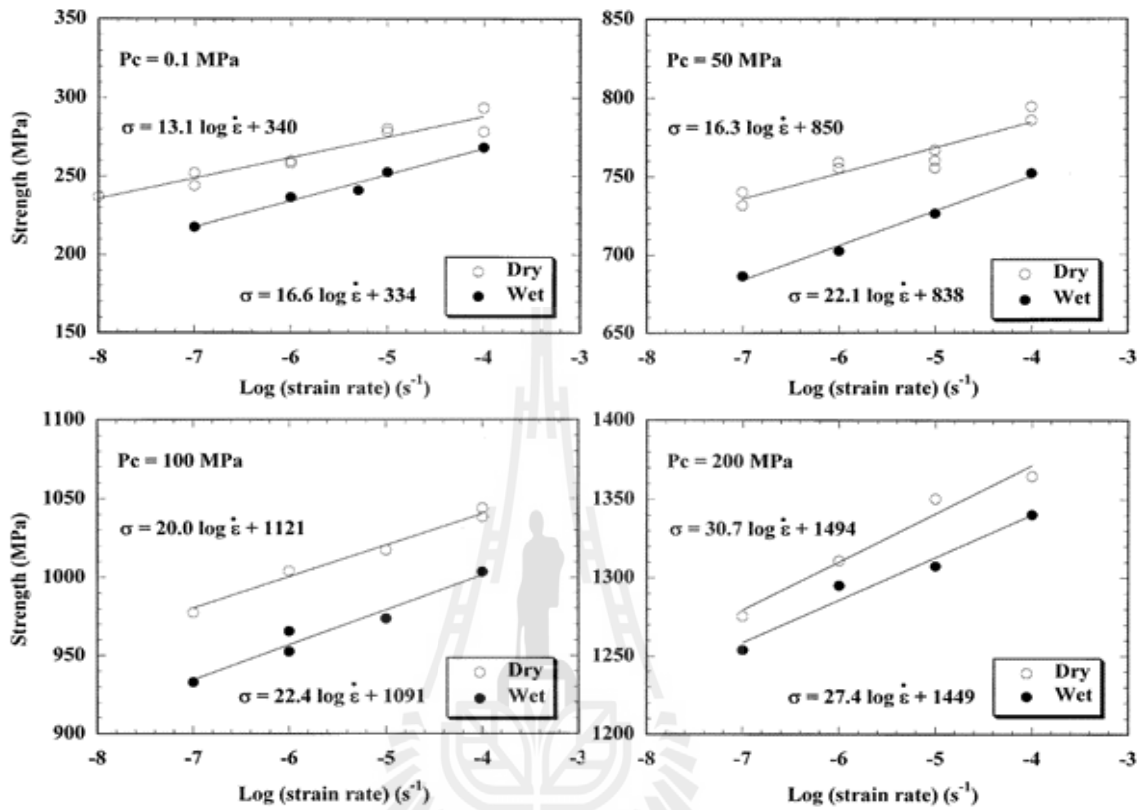


Figure 2.5 Compressive strength of granitic rocks as a function of strain rates under the varied confining pressures (Masuda, 2001).

2.3 Conclusion of review

The pore pressure can reduce the strength of rock. The rock compressive strengths decrease significantly as the water content increases. In term of deformability, the pore pressure is also reflected as a reduction of Young's modulus and increase of Poisson's ratio, which indicates that the saturated rocks will deform more than that of the dry ones under the same stress condition.

CHAPTER III

SAMPLE PREPARATION

3.1 Introduction

The tested sandstones are from three sources: Phra Wihan, Phu Phan and Phu Kradung sandstone formations (hereafter designated as PW, PP and PK sandstones). These rocks are classified as fine-grained quartz sandstones with highly uniform texture and density. These brittle rocks are medium strong. Their mechanical properties play a significant role in the stability of tunnels, slope embankments and dam foundations in the north and northeast of Thailand.

3.2 Sample preparation

Sample preparations are carried out in the laboratory at the Suranaree University of Technology. Specimens for the uniaxial and triaxial tests are prepared to obtain rectangular blocks with nominal dimensions of $50 \times 50 \times 100 \text{ mm}^3$ (Figure 3.1). A minimum of 40 specimens are prepared for each test and each rock types. The specimens are cut and ground to obtain the perpendicularity and parallelism to comply with the ASTM (D 4543) standard practice. They are prepared to test under dry and fully saturated conditions. Under dry condition the specimens are oven dried for 24 hours before testing. Under saturated condition the specimens are submersed under water using pressure vacuum chamber for 24 hours (Figure 3.2). Table 1 summarizes the physical properties of the rock samples. The saturated water content for PW, PP and PK sandstone can be determined as 4.9%, 2.1% and 1.5% using ASTM (D 2216-10) method. The PW, PP and PK sandstones show effective porosity of about 11%, 5% and 4%. The porosity can determine by using equation

$n = [(W-D)/V] \times 100$ (ASTM C830 – 00(2011)) where n is porosity, W is the saturated weight, D is the dry weight and V is the total bulk volume of specimen.

Table 1 The physical properties of tested sandstones.

Properties	PW	PP	PK
Dry density, ρ_{dry} (g/cc)	2.25 ± 0.06	2.42 ± 0.05	2.53 ± 0.03
Saturated density, ρ_{sat} (g/cc)	2.36 ± 0.04	2.47 ± 0.04	2.57 ± 0.02
Saturated water content, w (%)	4.91 ± 0.38	2.05 ± 0.22	1.53 ± 0.38
Effective porosity, n (%)	11.00 ± 0.97	4.97 ± 0.51	3.88 ± 0.98

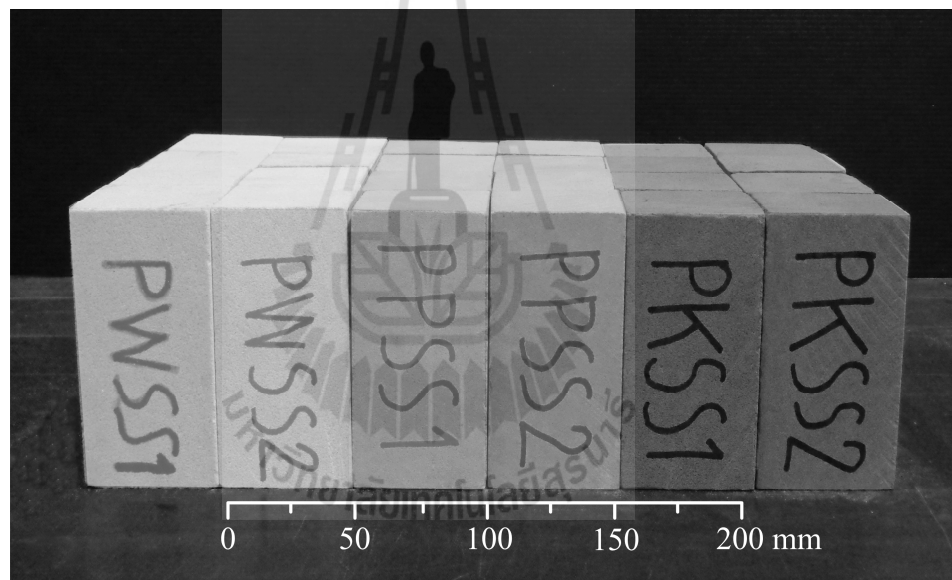


Figure 3.1 The rectangular block specimens of PW, PP and PK sandstones used in the uniaxial and triaxial testing are cut and ground to have a nominal dimension of $50 \times 50 \times 100 \text{ mm}^3$.

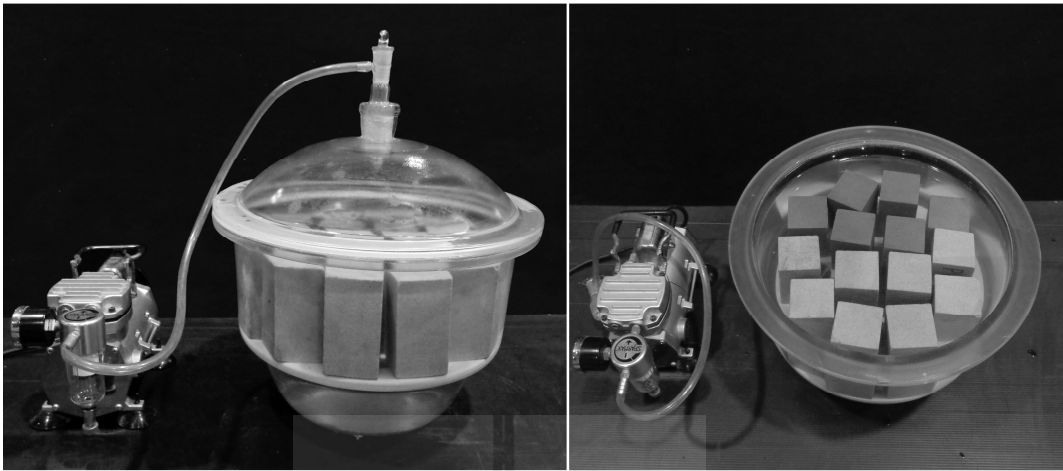


Figure 3.2 Sandstone specimens submersed under water in vacuum chamber.



CHAPTER IV

LABORATORY EXPERIMENTS

4.1 Introduction

The objective of the laboratory experiments is to assess the effects of pore pressure on the compressive strength and elasticity of the sandstone specimens. This chapter describes the method and results of the laboratory experiments. The tests are divided into two groups; rate-controlled uniaxial compression tests and rate-controlled triaxial compression tests.

4.2 Rate-controlled uniaxial compression tests

The objective of the rate-controlled uniaxial compression tests is to determine the ultimate strength and the deformability of the dry and saturated specimens under uniaxial load at various loading rates. The test procedures follow the American Society for Testing and Materials (ASTM D 7012-07) and the suggested methods by ISRM (Bieniawski and Bernede, 1978). The tests are performed by applying uniform axial stress under constant rate to the rectangular rock specimen and measuring the increase of axial strains as a function of time (Figure 4.1). The specimens are loaded failure under stress rates varying from 0.01, 0.1, 1 to 10 MPa/s. The post-failure characteristics are observed and recorded.

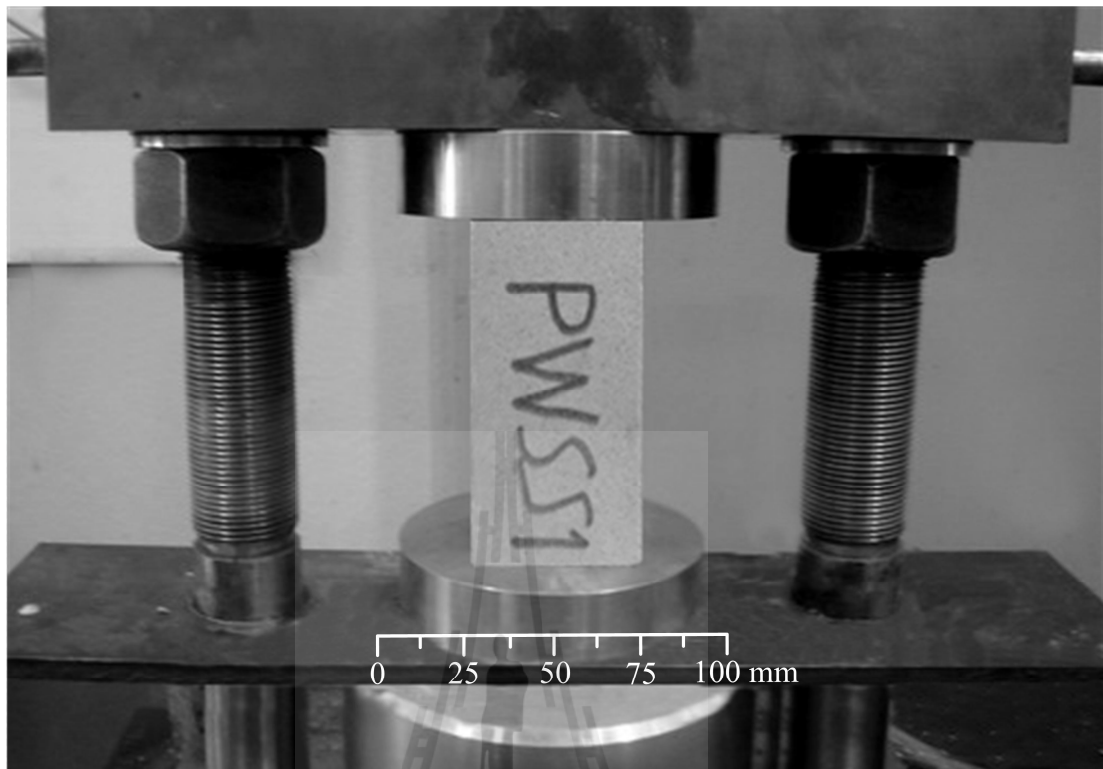


Figure 4.1 PW sandstone specimen placed under rate-controlled uniaxial load frame.

4.3 Rate-controlled triaxial compression tests

The objective of the rate-controlled triaxial compression test is to determine the effects of pore pressure on the compressive strength of the three sandstones under various confining pressures. The confining pressures range from 3, 7 to 12 MPa, and the constant axial stress rates from 0.001, 0.01, 0.1, 1.0 to 10 MPa/s. The specimen deformations monitored in the three principal directions are used to calculate the principal strains during loading. The failure stresses are recorded and mode of failure examined.

The polyaxial load frame has been used in this study because the cantilever beams with pre-calibrated dead weight can apply a truly constant lateral stress (confining pressure) to the specimen. Figure 4.2 shows the polyaxial load frame (Walsri et al., 2009). These lateral confining mechanism and deformation measurements are isolated from the axial

loading system. Such arrangement is necessary particularly for the triaxial testing under very high loading rates. For example at the loading rate of 10 MPa/s the sandstone specimens can fail within 5-8 seconds. The induced specimen dilation is too rapid for Hoek cell or triaxial cell to release the pressurized oil and maintain a constant confining pressure during loading. The excess oil pressure due to rapid dilation could lead to an error of the strength results.

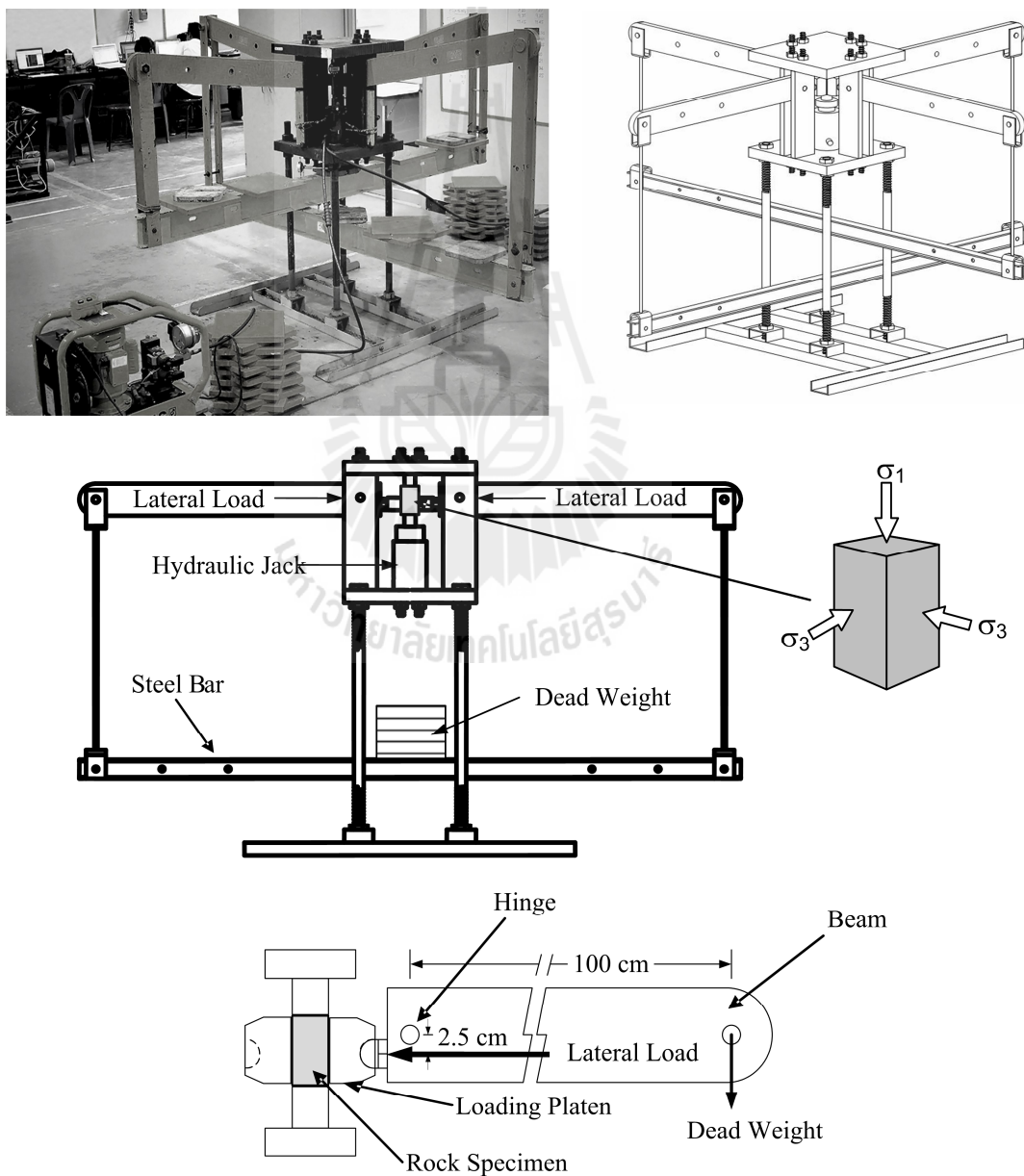


Figure 4.2 A polyaxial load frame used for the rate-controlled triaxial compressive strength tests.

4.4 Test results

Tables 4.1 through 4.3 summarize the test results for PW, PP and PK sandstones. Figure 4.3 plots the axial stress-strain curves obtained from the uniaxial tests under various loading rates for the three sandstones. The strengths of the dry specimens are always greater than those of the saturated specimens. The differences in strengths between the saturated and dry sandstones depend on the loading rate and confining pressure. The rock porosity also affects the strengths of saturated specimens. The rock specimens with higher porosity (PW sandstone) yield more different strengths between the saturated and dry conditions than those with a lower porosity (PP and PK sandstones). Figures 4.4 through 4.6 give the triaxial compression test results for the loading rates ($\delta\sigma_1/\delta t$) of 0.001, 0.01, 0.1 and 1 MPa/s with confining pressures varying from 3, 7 to 12 for the three sandstones. The tangent elastic moduli and Poisson's ratio at 50% failure stress have been calculated from the measured stress-strain curves obtained from all uniaxial and triaxial testing. Figures 4.7 and Figure 4.8 plotted the elastic moduli and Poisson's ratio as a function of the stress rate ($\delta\sigma_1/\delta t$). The elastic moduli and Poisson's ratio determined for both saturated and dry conditions increase with loading rate which can be best represented by a power equation for the elastic moduli and by a logarithmic equation for the Poisson's ratio as:

$$E = \kappa (\delta\sigma_1/\delta t)^\xi \quad (4.1)$$

$$v = A \cdot \log(\delta\sigma_1/\delta t) + B \quad (4.2)$$

where κ , ξ , A and B are empirical constants. The influence of pore pressure on the rock deformability is reflected as the reduction of Young's modulus (Figure 4.7) and the increase of the Poisson's ratio (Figure 4.8). The difference of the elastic moduli and Poisson's ratio under dry and saturated conditions increases with the loading rates.

Under lower loading rate of 0.001 MPa/s the elastic and Poisson's ratio are similar. This suggests that the pore pressure has no effect on the rock strengths if there is sufficient time to allow water to flow out of the specimens.

Based on the Coulomb strength criterion the cohesion (c) and internal friction angle (ϕ) of the rocks have been calculated (Table 4.4). The cohesions for both dry and saturated conditions are similar (Figure 4.9). The internal friction angle measured under saturated condition is lower than those under the dry condition (Figure 4.10). Both the internal friction angle and cohesion of the rocks increase with increasing loading rate which can be represented by the following equations:

$$\phi = \alpha \cdot \log(\delta\sigma_1/\delta t) + \beta \quad (4.3)$$

$$c = \psi \cdot \log(\delta\sigma_1/\delta t) + \omega \quad (4.4)$$

where α , β , ψ and ω are empirical constants.

Table 4.1 Summary of test results of Phra Wihan sandstone.

Confining pressure (MPa)	Loading Rate (MPa/s)	Compressive Strength, σ_c (MPa)		Elastic Modulus, E (GPa)	
		Dry	Sat.	Dry	Sat.
0	10	79	66	N/A	N/A
	1	67	60	11.8	10
	0.1	54	51	9.5	9.3
	0.01	48	48	8	7.9
	0.001	41	39	6.7	6.2
3	10	103	80	N/A	N/A
	1	86	76	12	10.2
	0.1	73	70	9.8	9.4
	0.01	65	63	8.1	8.7
	0.001	53	51	6.6	6.6
7	10	134	105	N/A	N/A
	1	120	103	11.6	10
	0.1	103	95	10.3	9
	0.01	87	86	8.5	8.4
	0.001	71	69	6.8	6.5
12	10	178	130	N/A	N/A
	1	154	130	12.5	9.8
	0.1	130	118	10	8.9
	0.01	120	110	8.2	7.8
	0.001	100	95	7.1	6.8

Table 4.2 Summary of test results of Phu Phan sandstone.

Confining pressure (MPa)	Loading Rate (MPa/s)	Compressive Strength, σ_c (MPa)		Elastic Modulus, E (GPa)	
		Dry	Sat.	Dry	Sat.
0	10	93	87	N/A	N/A
	1	85	82	13.7	13.4
	0.1	80	79	11.1	10.8
	0.01	76	74	8.4	8.2
	0.001	68	67	7.1	6.8
3	10	121	106	N/A	N/A
	1	108	100	13.5	12.6
	0.1	98	94	12.2	11.3
	0.01	93	91	9.3	9.3
	0.001	87	85	7.5	7.5
7	10	142	127	N/A	N/A
	1	131	124	12.6	12.6
	0.1	118	114	11.4	10.3
	0.01	110	107	8.8	8.8
	0.001	104	102	8.2	8
12	10	167	152	N/A	N/A
	1	157	147	13.3	12
	0.1	146	139	12.3	11
	0.01	138	133	8.4	8.1
	0.001	130	127	7.6	7.2

Table 4.3 Summary of results of Phu Kradung sandstone.

Confining pressure (MPa)	Loading Rate (MPa/s)	Compressive Strength, σ_c (MPa)		Elastic Modulus, E (GPa)	
		Dry	Sat.	Dry	Sat.
0	10	80	77	N/A	N/A
	1	74	72	10.8	10
	0.1	65	64	9.5	8.9
	0.01	58	57	8	7.4
	0.001	46	45	6.5	6.2
3	10	103	94	N/A	N/A
	1	95	90	11	9.8
	0.1	83	80	9	8.6
	0.01	75	72	7.4	7.5
	0.001	65	59	6.7	5.8
7	10	130	116	N/A	N/A
	1	120	112	10.8	10.3
	0.1	105	102	9.6	8.6
	0.01	97	92	7.9	6.9
	0.001	80	77	7.1	6.3
12	10	161	145	N/A	N/A
	1	152	140	11	9.6
	0.1	134	130	8.9	8.7
	0.01	123	117	7.4	7.1
	0.001	106	100	6.8	6.1

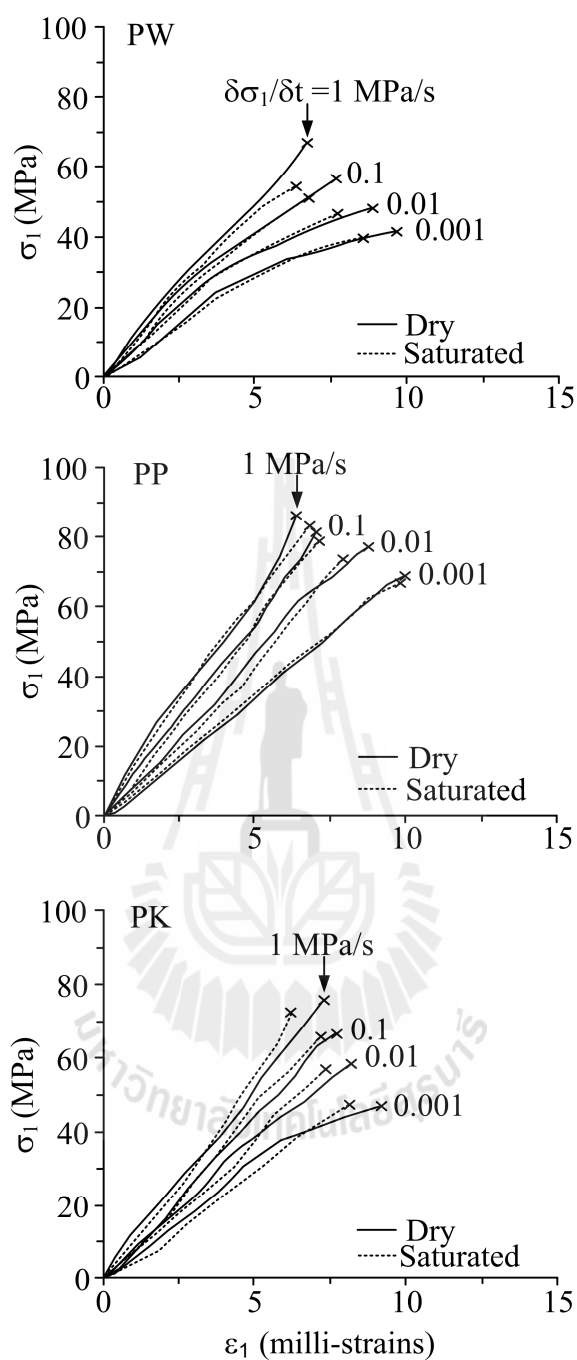


Figure 4.3 Uniaxial compressive stresses and strains with loading rates varied from 0.001, 0.01, 0.1 and 1.0 MPa/s, for PW, PP and PK sandstones under dry and saturated conditions.

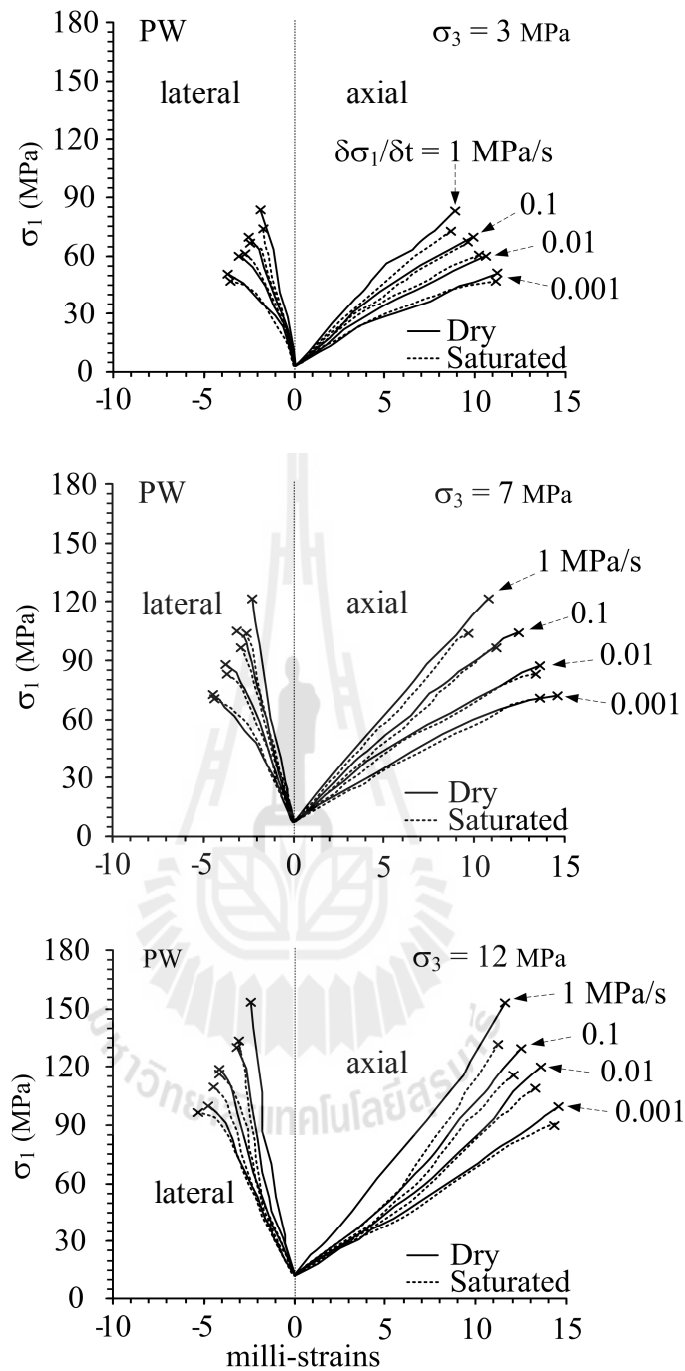


Figure 4.4 Triaxial compressive stresses and strains for PW sandstone for the loading rates ($\delta\sigma_1/\delta t$) of 0.001, 0.01, 0.1 and 1 MPa/s and confining pressures varying from 3, 7 to 12 MPa.

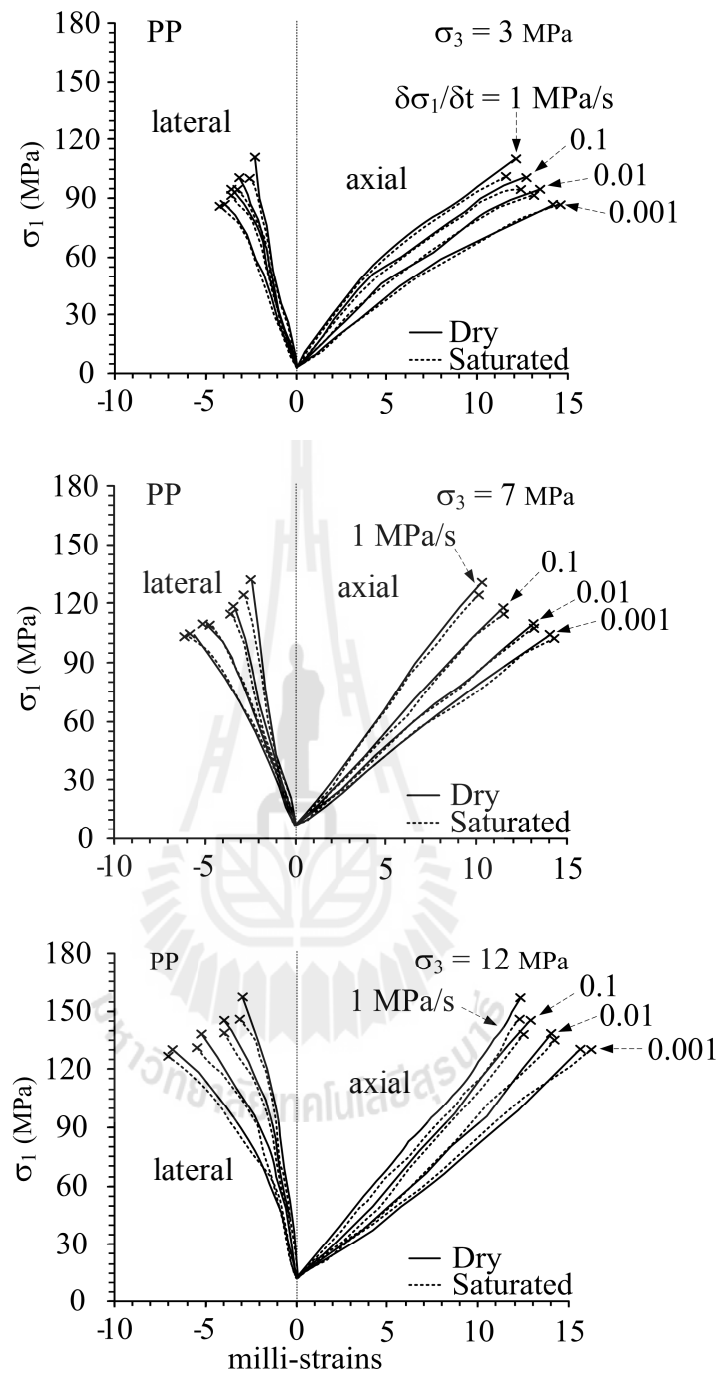


Figure 4.5 Triaxial compressive stresses and strains for PP sandstone for the loading rates ($\delta\sigma_1/\delta t$) of 0.001, 0.01, 0.1 and 1 MPa/s and confining pressures varying from 3, 7 to 12 MPa.

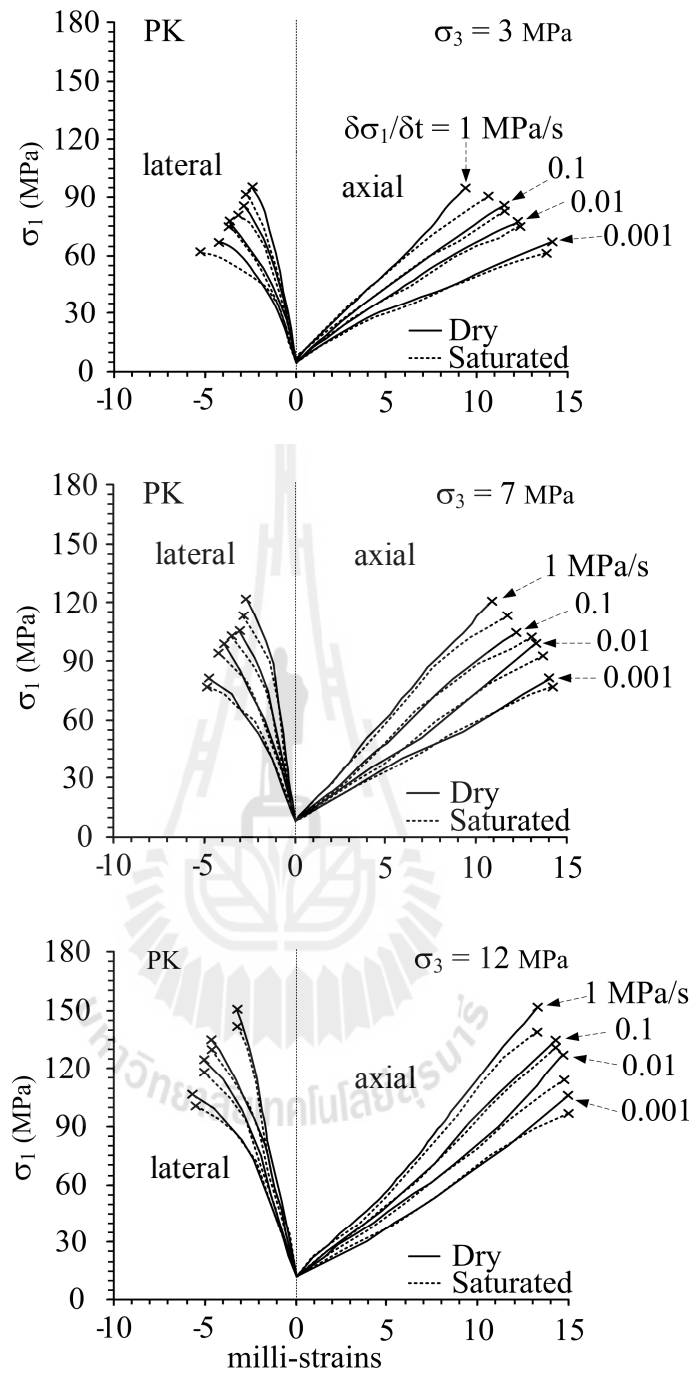


Figure 4.6 Triaxial compressive stresses and strains for PK sandstone for the loading rates ($\delta\sigma_1/\delta t$) of 0.001, 0.01, 0.1 and 1 MPa/s and confining pressures varying from 3, 7 to 12 MPa.

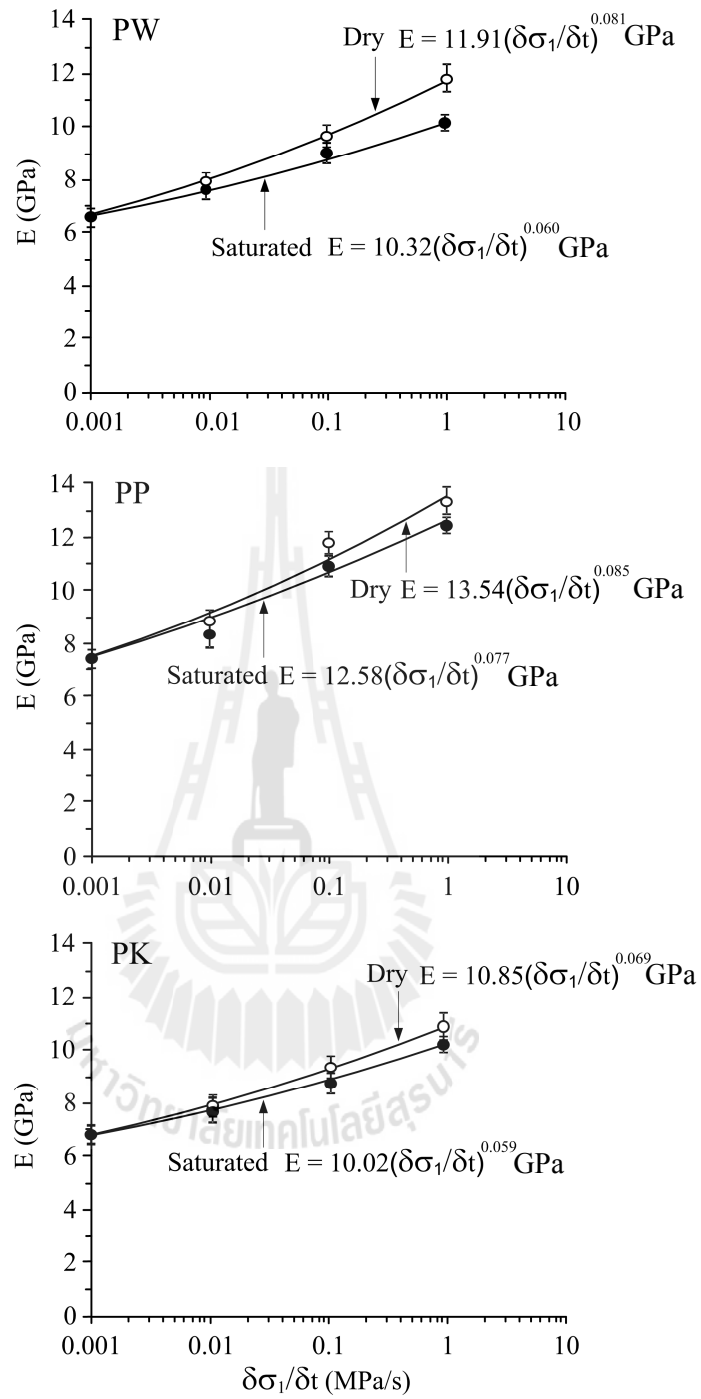


Figure 4.7 Elastic modulus (E) as a function of applied loading rate ($\delta\sigma_1/\delta t$) for PW, PP and PK sandstones.

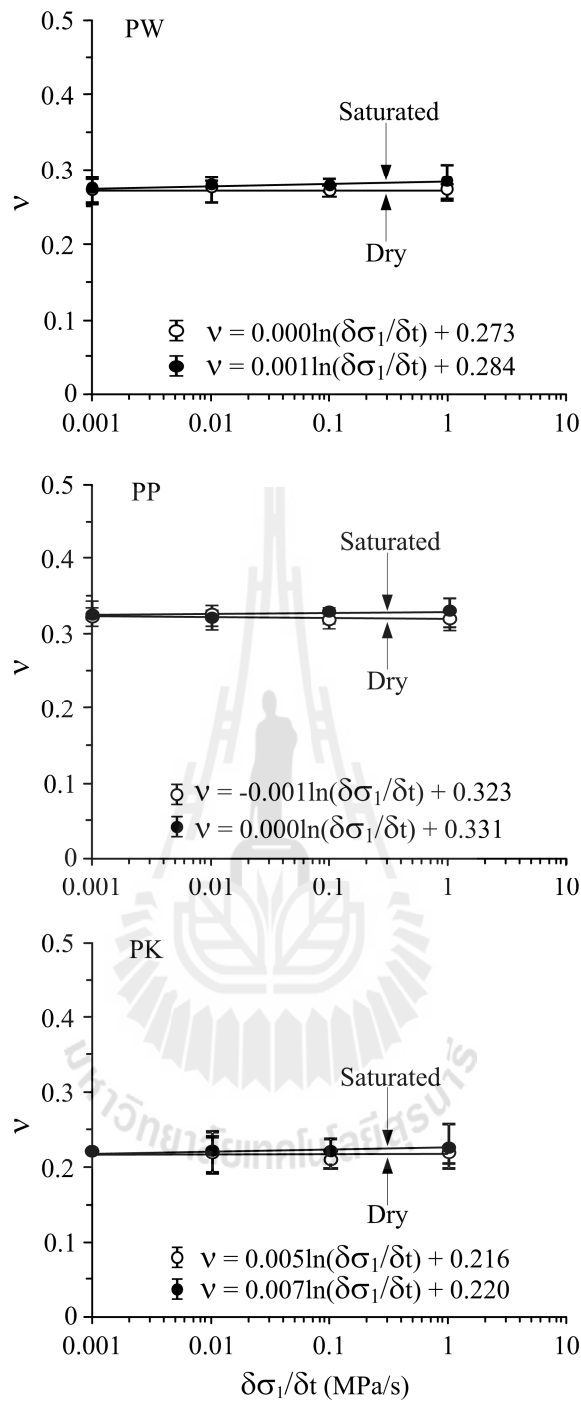


Figure 4.8 Poisson ratio (ν) as a function of applied loading rates ($\delta\sigma_1/\delta t$) for dry and saturated specimens.

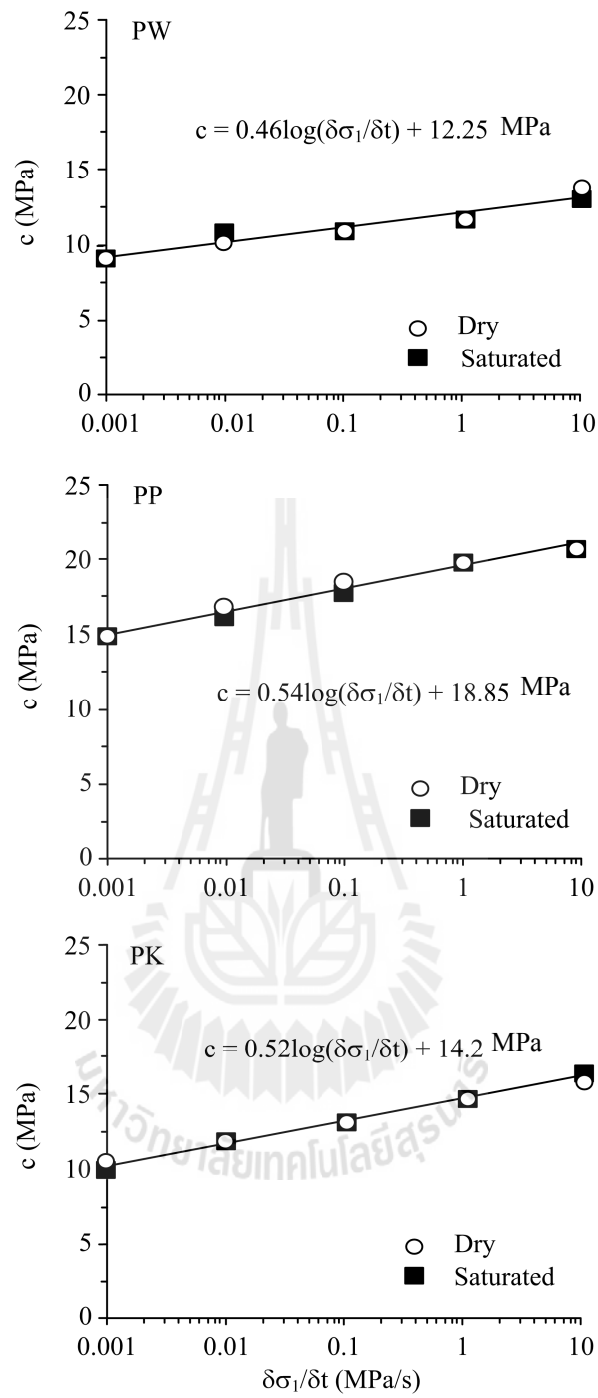


Figure 4.9 Cohesion (c) as a function of applied loading rate ($\delta\sigma_1/\delta t$) for dry and saturated specimens.

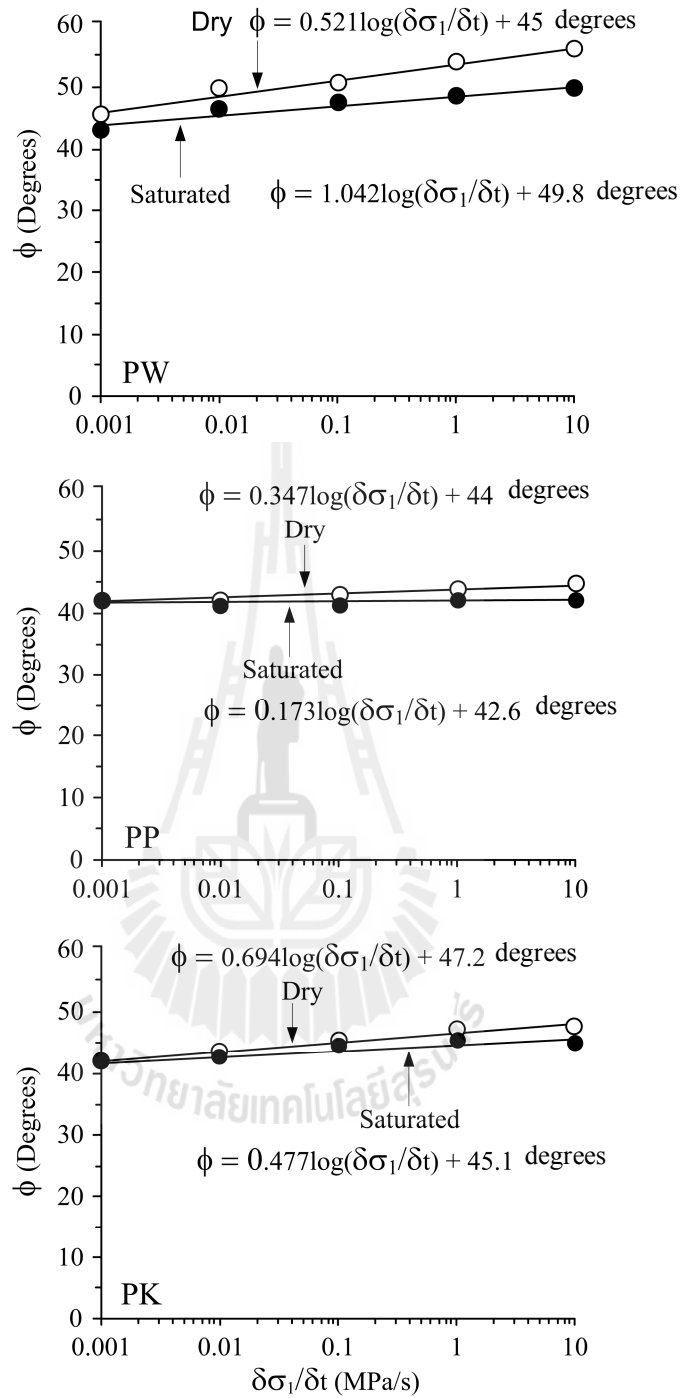


Figure 4.10 Friction angles (ϕ) as a function of applied loading rates $\delta\sigma_1/\delta t$ for dry and saturated specimens.

CHAPTER V

ANALYSIS

5.1 Introduction

The objective of this chapter is to compare the strength and elastic results between dry and saturated conditions. The results have been studied to determine the effects of pore pressure on compressive strength and elastic properties of three sandstones. The results obtained have are also compared with other researches.

5.2 Effect of pore pressure on strength

Figures 5.1 through 5.3 show the compressive strengths of the sandstone under confining pressures for dry and saturated conditions. The compressive strength increased with confining pressures and loading rates. This agrees with the results obtained by Kenkhunthod and Fuenkajorn (2009). The increase is observed under both dry and saturated conditions. The strengths of the dry specimens are higher than those of the saturated specimens for the same confining pressure and the stress rates. The difference in strengths between the saturated and dry sandstones ($\Delta = (\sigma_{\text{dry}} - \sigma_{\text{sat}}) / \sigma_{\text{dry}}$) varies from 1 to 27 percents depending on the loading rate and confining pressure (Table 5.1). This trend of variation is more obvious for PW sandstone, particularly at the stress rates of 1 MPa/s and 10 MPa/s.

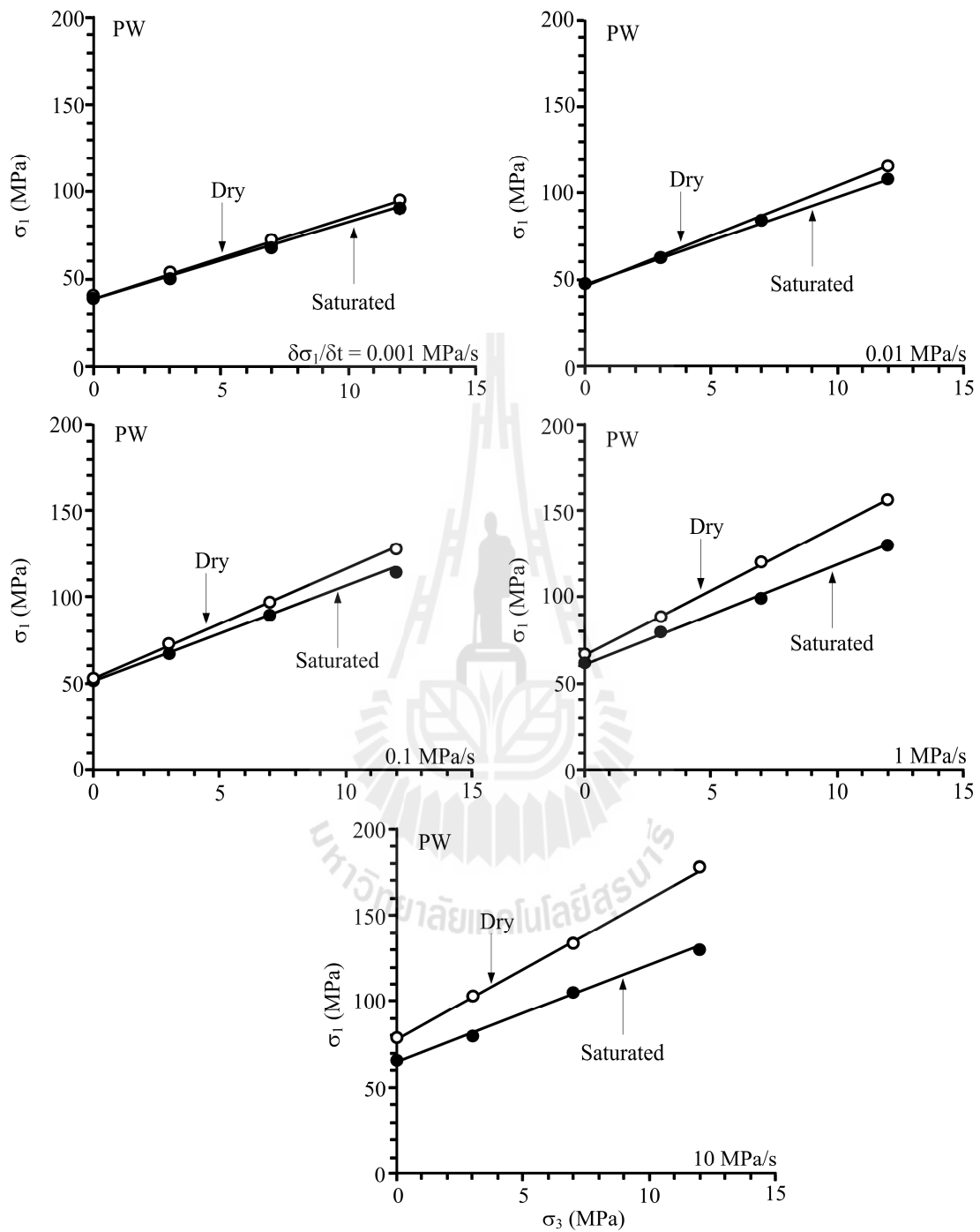


Figure 5.1 Maximum principal stress (σ_1) as a function of minimum principal stress (σ_3) at failure various loading rates for dry and saturated conditions for PW sandstone.

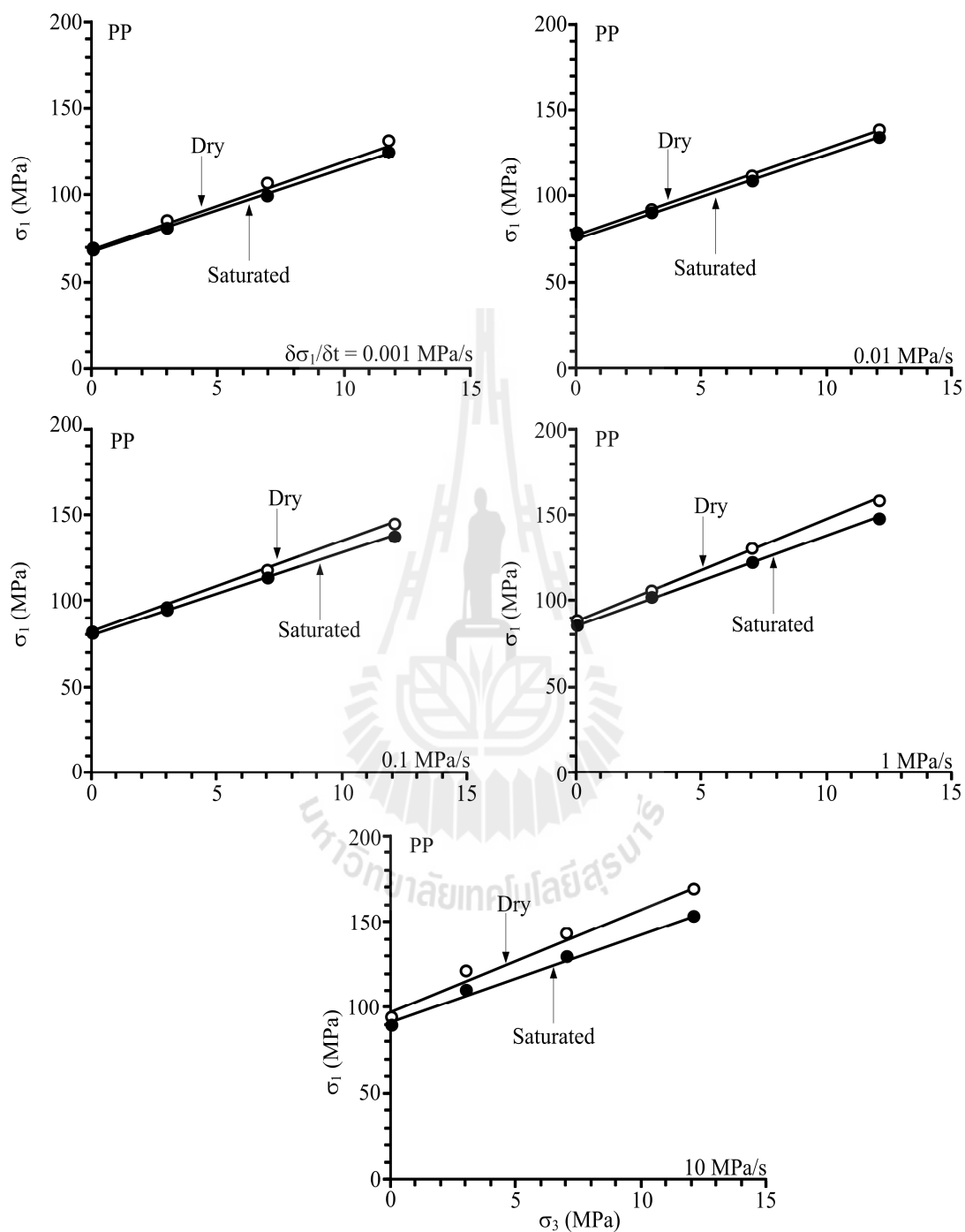


Figure 5.2 Maximum principal stress (σ_1) as a function of minimum principal stress (σ_3) at failure various loading rates for dry and saturated conditions for PP sandstone.

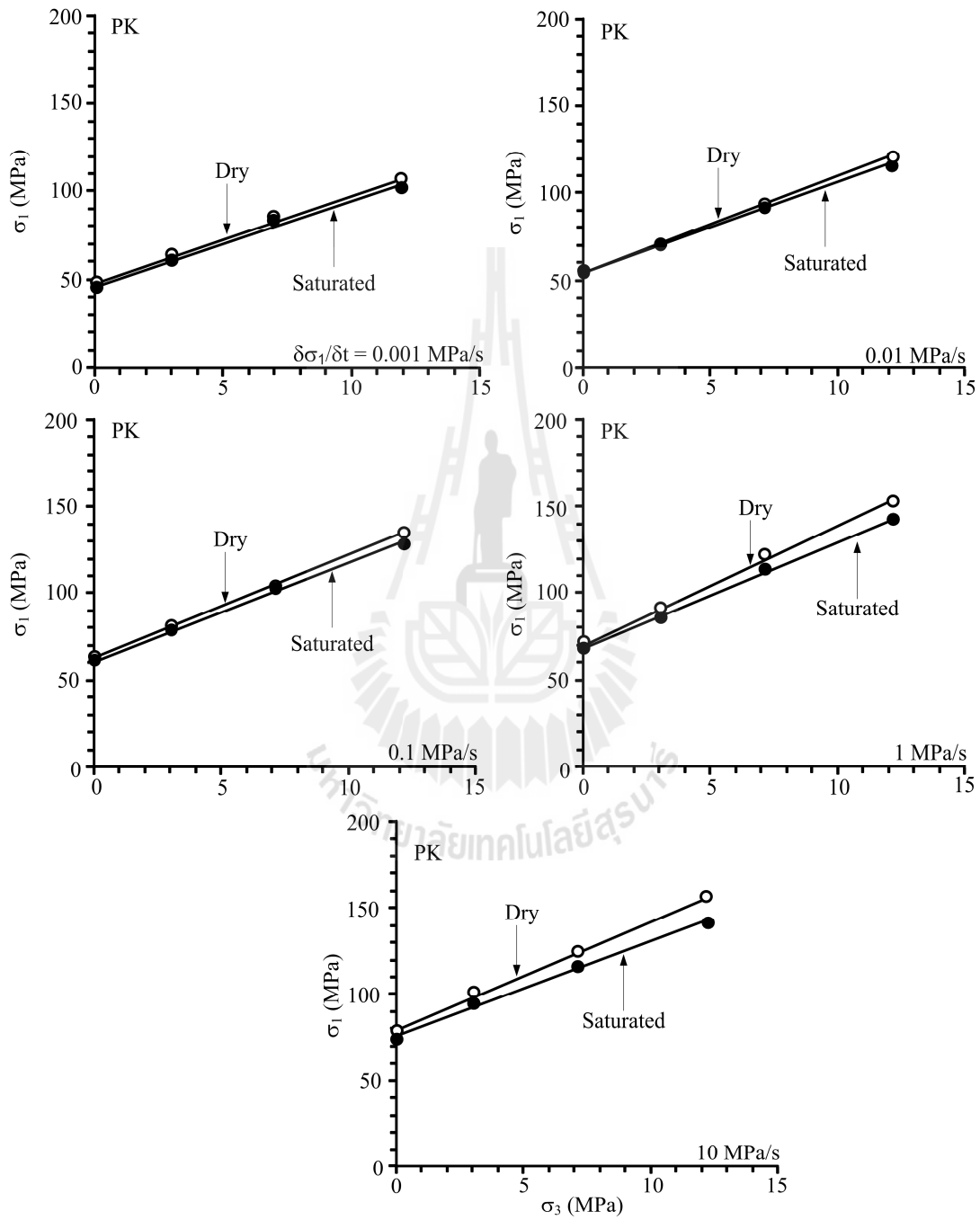


Figure 5.3 Maximum principal stress (σ_1) as a function of minimum principal stress (σ_3) at failure various loading rates for dry and saturated conditions for PK sandstone.

Table 5.1 Summary of the strength results.

σ_3 (MPa)	$\delta\sigma_1/\delta t$ (MPa/s)	PW σ_1 (MPa)			PP σ_1 (MPa)			PP σ_1 (MPa)		
		Dry	Sat.	Δ (%)	Dry	Sat.	Δ (%)	Dry	Sat.	Δ (%)
0	0.001	41	39	4.9	46	44	4.3	68	67	1.5
	0.01	48	48	0.0	54	53	1.9	76	74	2.6
	0.1	54	51	5.6	61	59	3.3	80	79	1.3
	1	67	60	10.4	71	68	4.2	85	82	3.5
	10	79	66	16.5	80	75	6.3	93	89	4.3
3	0.001	53	51	3.8	65	62	4.6	87	85	2.3
	0.01	65	63	3.1	73	72	1.4	93	91	2.2
	0.1	73	70	4.1	84	80	4.8	98	96	2.0
	1	86	76	11.6	90	87	3.3	108	104	3.7
	10	103	80	22.3	101	97	4.0	121	110	9.1
7	0.001	71	69	2.8	86	83	3.5	104	100	3.8
	0.01	87	86	1.1	97	93	4.1	110	108	1.8
	0.1	103	95	7.8	105	102	2.9	118	114	3.4
	1	120	103	14.2	121	113	6.6	131	124	5.3
	10	134	105	21.6	130	121	6.9	142	129	9.2
12	0.001	100	95	5.0	106	103	2.8	130	127	2.3
	0.01	120	110	8.3	122	117	4.1	138	133	3.6
	0.1	130	118	9.2	134	129	3.7	146	139	4.8
	1	154	130	15.6	152	141	7.2	157	147	6.4
	10	178	130	27.0	161	145	9.9	167	152	9.0

5.3 Effect of pore pressure on elastic properties

The variation elastic modulus and the Poisson's ratio of the three rock types with confining pressures and loading rates under dry and saturated conditions have been presented in Chapter IV. For all sandstones tested here the elastic modulus exponentially decreases with the applied stress rates. It can be seen that the elastic modulus of saturated specimens are lower than those of dry at the same confining pressure and loading rates for the three rock types. This agrees with the results obtained by Kenkhunthod and Fuenkajorn (2009) and Li et al (2012). The average Poisson's ratios are 0.27, 0.32 and 0.22 of dry specimens for the PW, PP and PK sandstones, respectively. The Poisson's ratio of saturated specimen is larger than that of dry specimen at the same confining pressure and stress rates. The Poisson's ratio of saturated and dry specimen at 0.001 MPa/s is very close.

5.4 Mathematical determination

Terzaghi's effective stress law states that the pore pressure of a rock will cause the same reduction in peak stress as caused by reduction of the confining pressure by an amount (equal to P_w). The effective stress σ' is defined by (Goodman, 1989).

$$\sigma' = \sigma - P_w \quad (5.1)$$

The effect of pore pressure can be incorporated into in the failure criterion simply by restating the conditions for failure in terms of effective stresses. For dry rock, there is no difference between normal stresses and effective normal stresses.

In terms of the principal stresses at peak load conditions, the Mohr-Coulomb criterion can be written as:

$$\sigma_1 = \sigma_u + \sigma_3 \tan^2[45 + (\phi/2)] \quad (5.2)$$

where σ_1 is the major principal stress, σ_3 is the confining pressures and σ_u is the uniaxial compressive strength. For a saturated rock, equation (5.2) in terms of effective stress becomes:

$$\sigma'_1 - \sigma'_3 = \sigma_u + [\sigma'_3 \tan^2(45 + \phi/2) - 1] \quad (5.3)$$

Since the differential stress is unaffected by pore pressure, equation (5.3) becomes:

$$\sigma_1 - \sigma_3 = \sigma_u + (\sigma_3 - P_w)[\tan^2(45 + \phi/2) - 1] \quad (5.4)$$

Solving for P_w , equation (5.4) can be rewritten as:

$$P_w = \sigma_3 - [(\sigma_1 - \sigma_3) \sigma_u] / [\tan^2(45 + \phi/2) - 1] \quad (5.5)$$

Table 5.2 summarizes the effective stress and pore water pressure of PW, PP and PK sandstones under various loading rates and confining pressures. The pore pressure begins to affect when loading rates increase from 0.1 to 10 MPa/s (Figure 5.4). The high porosity PW sandstone shows more effect of pore pressure than do the low porosity PP and PK sandstones.

Table 5.2 Effective stresses and pore pressures of PW, PP and PK sandstones.

σ_3 (MPa)	$\delta\sigma_1/\delta t$ (MPa/s)	PW			PP			PP		
		P_w (MPa)	σ'_3 (MPa)	σ'_1 (MPa)	P_w (MPa)	σ'_3 (MPa)	σ'_1 (MPa)	P_w (MPa)	σ'_3 (MPa)	σ'_1 (MPa)
0	0.001	0.4	0	38.6	0.1	0	66.1	0.3	0	44.7
	0.01	0	0	48	0.3	0	73.0	0.2	0	56.8
	0.1	0.2	0	50.3	0.3	0	78.3	0.4	0	63.6
	1	1	0	59	0.4	0	81.7	0.4	0	71.6
	10	2.5	0	63.5	0.5	0	85.9	0.5	0	76.5
3	0.001	0.4	2.6	51.6	0.2	2.8	85.9	0.2	2.8	58.8
	0.01	0.5	2.5	62.5	0.3	2.7	91.1	0.3	2.7	71.7
	0.1	0.3	2.7	70	0.4	2.6	93.7	0.5	2.5	79.7
	1	1	2	75	0.4	2.6	99.8	0.3	2.7	89.7
	10	3.2	0	76.8	0.6	2.4	105.4	0.8	2.2	93.2
7	0.001	0.2	6.8	69.2	0.2	6.8	102.5	0.1	6.7	76.7
	0.01	0.4	6.6	83.6	0.3	6.7	106.3	0.3	6.7	91.7
	0.1	0.5	6.5	92	0.4	6.6	113.9	0.6	6.4	101.6
	1	1.2	5.8	103	0.7	6.3	124.5	0.6	6.4	111.4
	10	3.8	3.2	103	1.1	5.9	125.7	1.2	5.8	114.8
12	0.001	0.3	11.7	95	0.3	11.7	128.6	0.3	11.7	99.7
	0.01	0.5	11.5	109.5	0.2	11.8	133.0	0.4	11.6	116.6
	0.1	0.6	11.4	120	0.4	11.6	138.6	0.7	11.3	128.8
	1	1.4	10.6	135	0.8	11.2	146.0	0.8	11.2	139.2
	10	4.4	7.6	126	1.5	10.5	150.5	1.5	10.5	143.8

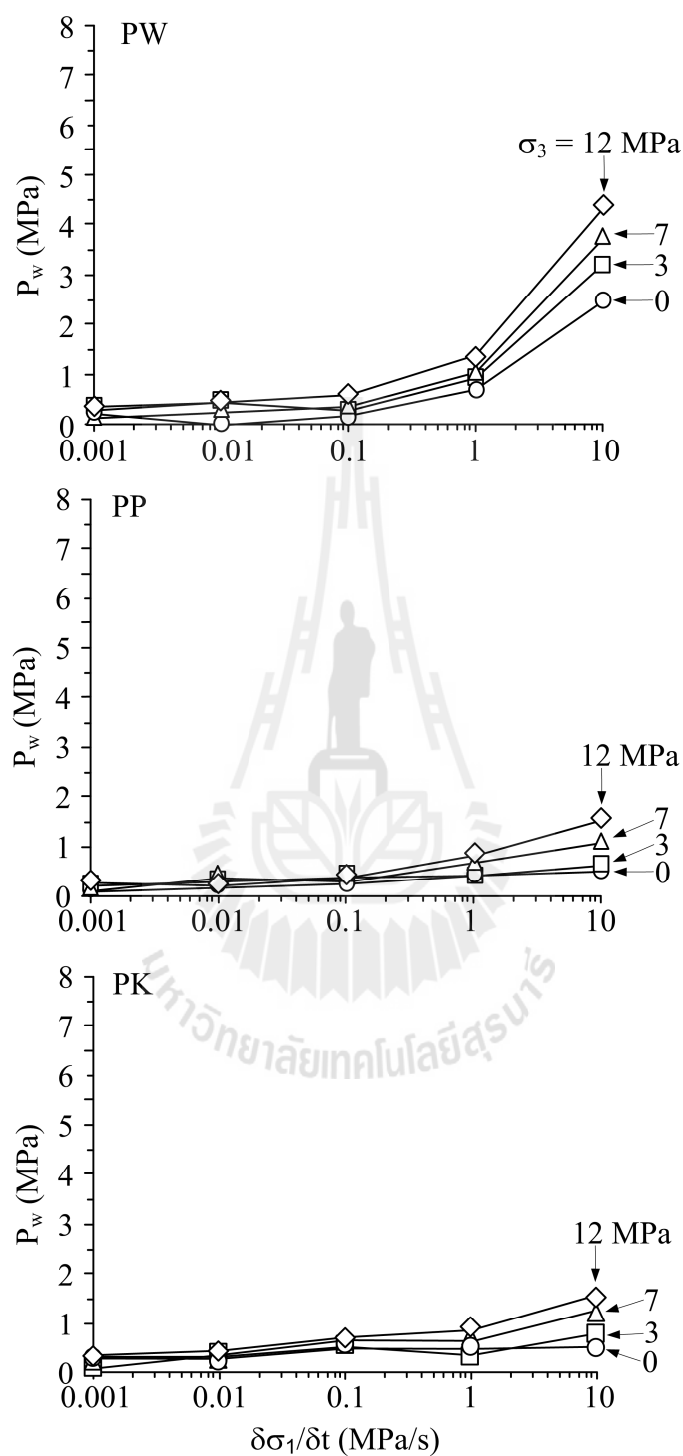


Figure 5.4 Pore pressures (P_w) as a function of applied loading rates ($\delta\sigma_1/\delta t$) for saturated specimens.

CHAPTER VI

DISCUSSIONS, CONCLUSIONS, AND RECOMMENDATIONS FOR FUTURE STUDIES

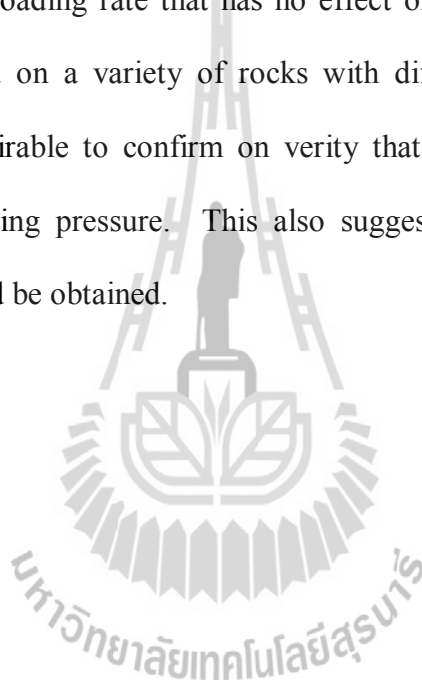
6.1 Discussions and conclusions

The test results indicate that the pore pressure can reduce the strength of rock which agree well with several researches conducted elsewhere (Masuda, 2001; Peng and Zhang, 2007; Sun and Hu, 1997; Li and Reddish, 2004). The decrease of compressive strengths of saturated rock depends on the loading rate and confining pressure. The effect of pore pressure on deformability of rocks is reflected as a reduction of elastic modulus and increase of Poisson's ratio. The pore pressure depends on the water content and porosity. The higher porosity results in a higher pore pressure (Talesnick and Shehadeh, 2006).

A method for estimating the pore pressure of the three sandstones has been presented. A new triaxial testing device was developed which enables to carry out axial stress controlled tests on rock specimens under loading rates ranging from 0.001 to 10 MPa/s. The tested results indicate that the polyaxial load frame perform well for the assessment of the effects of pore pressure on the compressive strength of the sandstones. On the basis of corresponding test results on rock specimens loading rate dependent formulations of both deformability and shear strength have been developed. From an analysis of the results of Terzaghi's effect stress law and Mohr-Coulomb criterion, the pore pressure is found to be dependent on the porosity and the loading rate. Here the pore pressure can significantly reduce the compressive strength up to 1 to 27 percent depending on the loading rates and confining pressure. This effect pronounces more under greater confining pressures. The findings are useful for predicting the strength of in-situ rocks under saturation and subject to loading rates that are different from those used in the laboratory.

6.2 Recommendations for future studies

The uncertainties of the studied investigation and results discussed above lead to the recommendations for further studies. The test should be to directly measure the pressure changes in the specimen. The results can be compared with the result obtained here for verification. Lower loading rates of less than 0.001 MPa/s are also desirable to find the lower bound of the loading rate that has no effect on the pore pressure and strength. More testing is required on a variety of rocks with different porosity volumes. More investigation is also desirable to confirm on verity that the effect of pore pressure acts equally under all confining pressure. This also suggests that test results under higher confining pressure should be obtained.



REFERENCES

- ASTM C830-00 (2011). Standard Test Methods for Apparent Porosity, Liquid Absorption, Apparent Specific Gravity, and Bulk Density of Refractory Shapes by Vacuum Pressure. In **Annual Book of ASTM Standards**. (Vol. 15.01). American Society for Testing and Materials: Philadelphia.
- ASTM D2216-10. Standard Test Methods for Laboratory Determination of Water (Moisture) Content of Soil and Rock by Mass. In **Annual Book of ASTM Standards**. (Vol. 04.08). American Society for Testing and Materials: Philadelphia.
- ASTM D4543-85. Standard practice for preparing rock core specimens and determining dimensional and shape tolerances. In **Annual Book of ASTM Standards**. (Vol. 04.08). American Society for Testing and Materials: Philadelphia.
- ASTM D7012-07. Compressive strength and elastic moduli of intact rock core specimens under varying states of stress and temperatures. In **Annual Book of ASTM Standards**. (Vol. 04.08). American Society for Testing and Materials: Philadelphia.
- Bieniawski, Z.T. and Bernede, M.J. (1978). Suggested methods for determining the uniaxial compressive strength and deformability of rock materials. **International Journal of Rock Mechanics and Mining Sciences** 16(2): 138-140.
- Chang, C. and Haimson, B. (2007). Effect of fluid pressure on rock compressive failure in a nearly impermeable crystalline rock: Implication on mechanism of borehole breakouts. **Engineering Geology** 89(3-4): 230-242.

- Fredrich, J.T., Martin, J.W. and Clayton, R.B. (1995). Induced pore pressure response during undrained deformation of tuff and sandstone. **International Journal of Mechanics of Materials** 20: 95-104.
- Goodman, R.E. (1989). **Introduction to rock mechanics**. JohnWiley & Sons, New York.
- Hawkins, A.B. and McConnell, B. J. (1992). Sensitivity of sandstone strength and deformability to changes in moisture content. **Engineering Geology** 25: 115-130.
- Kenkhunthod, N. and Fuenkajorn, K. (2009). Loading rate effects on strength and stiffness of sandstones under confinement. In **Proceedings 2nd Thailand Symposium on Rock mechanics**. Chonburi, Thailand. 2: 271-282.
- Li, D., Wong, L.N.Y., Liu, G. and Zhang, X. (2012). Influence of water content and anisotropy on the strength and deformability of low porosity meta-sedimentary rocks under triaxial compression. **Engineering Geology** 126: 46-66.
- Li, Z. and Reddish, D.J. (2004). The effect of groundwater recharge on broken rocks. **International Journal of Rock Mechanics and Mining Sciences** 41(3): 409.
- Masuda, K. (2001). Effects of water on rock strength in a brittle regime. **Journal of Structural Geology** 23(11): 1653-1657.
- Peng, S. and Zhang, J. (2007). **Engineering Geology for Underground Rocks**, Springer, New York: 342 p.
- Perera, M.S.A., Ranjith, P.G. and Peter, M. (2011). Effect of saturation medium and pressure on strength parameters of Latrobe Valley brown coal: Carbon dioxide, water and nitrogen saturations. **Energy** 36(12): 6941-6947.

- Sulem, J. and Ouffroukh, H. (2006). Shear banding in drained and undrained triaxial tests on a saturated sandstone: Porosity and permeability evolution. **International Journal of Rock Mechanics and Mining Sciences** 43(2): 292-310.
- Sun, J. and Hu, Y.Y. (1997). Time-dependent effects on the tensile strength of saturated granite at three gorges project in China. **International Journal of Rock Mechanics and Mining Sciences** 34(3-4): 306.e1-306.e13.
- Talesnick, M. and Shehadeh, S. (2006). The effect of water content on the mechanical response of a high-porosity chalk. **International Journal of Rock Mechanics and Mining Sciences** 44(4): 584-600.
- Tien, Y.M. Lee, D.H. Juang. and Strain, C.H. (1990). Pore pressure and fatigue characteristics of sandstone under various load conditions. **International Journal of Rock Mechanics and Mining Sciences** 27(4): 283-289.
- Vasarhelyi, B. (2003). Some observations regarding the strength and deformability of sandstones in case of dry and saturated conditions. **Geology Environment** 62: 245-249.
- Vasarhelyi, B. and Van, P. (2006). Influence of water content on the strength of rock. **Engineering Geology** 84: 70-74.
- Walsri, C., Poonprakon, P., Thosuwan, R. and Fuenkajorn, K. (2009). Compressive and tensile strengths of sandstones under true triaxial stresses. In **Proceedings 2nd Thailand Symposium on Rock mechanics**. Chonburi, Thailand. 2: 199-218.
- Yilmaz, I. (2010). Influence of water content on the strength and deformability of gypsum. **International Journal of Rock Mechanics and Mining Sciences** 42(2): 342-347.
- Yoshinaka, R. Tran, T.V. and Osada, M. (1997). Pore pressure changes and strength mobilization of soft rocks in consolidated-undrained cyclic loading triaxial tests. **International Journal of Rock Mechanics and Mining Sciences** 34(5): 715-726.



APPENDIX A

DIMENSIONS AND DENSITY OF SPECIMENS

มหาวิทยาลัยเทคโนโลยีสุรนารี

Table A.1 Dimensions and density of PW sandstone under dry condition.

Specimen no.	Width (mm)	Length (mm)	Height (mm)	Dry Density (g/cc)
PWSS-01	53.0	54.0	103.8	2.17
PWSS-02	53.5	53.0	104.0	2.19
PWSS-03	52.5	53.0	103.1	2.23
PWSS-04	52.4	53.4	103.8	2.23
PWSS-05	52.4	53.6	104.4	2.21
PWSS-06	52.3	53.3	103.7	2.22
PWSS-07	52.6	52.7	104.3	2.26
PWSS-08	52.5	53.2	103.8	2.25
PWSS-09	52.7	53.7	103.8	2.20
PWSS-10	52.2	52.5	104.1	2.22
PWSS-11	52.9	52.6	103.4	2.26
PWSS-12	52.1	52.3	103.4	2.31
PWSS-13	52.4	52.4	104.3	2.23
PWSS-14	52.3	52.4	104.3	2.23
PWSS-15	52.3	52.4	103.5	2.25
PWSS-16	53.4	52.0	103.1	2.23
PWSS-17	52.3	52.3	103.8	2.25
PWSS-18	52.3	52.5	104.4	2.23
PWSS-19	52.6	52.5	104.4	2.21
PWSS-20	53.0	52.4	103.4	2.25

Table A.2 Dimensions and density of PP sandstone under dry condition.

Specimen no.	Width (mm)	Length (mm)	Height (mm)	Dry Density (g/cc)
PPSS-01	50.50	53.64	101.42	2.38
PPSS-02	50.14	54.26	102.02	2.46
PPSS-03	51.10	50.80	101.74	2.46
PPSS-04	50.44	51.80	102.08	2.39
PPSS-05	50.40	51.30	101.84	2.41
PPSS-06	51.18	52.94	101.12	2.42
PPSS-07	50.40	53.04	101.28	2.46
PPSS-08	50.40	51.38	101.02	2.43
PPSS-09	50.72	51.30	102.48	2.30
PPSS-10	50.00	50.20	101.28	2.41
PPSS-11	50.18	51.00	102.06	2.43
PPSS-12	50.00	50.30	102.76	2.43
PPSS-13	50.40	51.78	101.10	2.37
PPSS-14	50.10	52.20	101.18	2.49
PPSS-15	50.00	51.00	101.38	2.40
PPSS-16	50.50	54.52	101.50	2.48
PPSS-17	50.70	51.18	101.58	2.43
PPSS-18	50.60	54.52	101.30	2.44
PPSS-19	49.42	53.20	101.68	2.48
PPSS-20	50.50	53.64	101.42	2.38

Table A.3 Dimensions and density of PK sandstone under dry condition.

Specimen no.	Width (mm)	Length (mm)	Height (mm)	Dry Density (g/cc)
PKSS-01	52.00	54.10	101.60	2.50
PKSS-02	51.62	53.90	101.78	2.52
PKSS-03	51.22	54.00	101.94	2.53
PKSS-04	52.98	51.48	101.80	2.56
PKSS-05	51.96	53.44	101.58	2.53
PKSS-06	54.00	51.60	101.82	2.53
PKSS-07	51.24	53.00	102.00	2.56
PKSS-08	51.60	54.14	101.98	2.53
PKSS-09	53.24	51.10	101.98	2.53
PKSS-10	53.00	51.90	102.18	2.53
PKSS-11	53.06	51.98	102.10	2.54
PKSS-12	51.58	53.80	101.72	2.54
PKSS-13	51.58	53.90	101.48	2.54
PKSS-14	51.60	53.64	101.96	2.54
PKSS-15	51.48	53.96	101.82	2.54
PKSS-16	51.78	53.92	101.98	2.54
PKSS-17	51.24	54.06	101.90	2.52
PKSS-18	51.94	52.26	101.88	2.55
PKSS-19	51.68	54.00	101.68	2.52
PKSS-20	51.38	53.86	101.80	2.52

Table A.4 Dimensions and density of PW sandstone under saturated condition.

Specimen no.	Width (mm)	Length (mm)	Height (mm)	Dry Density (g/cc)	Wet Density (g/cc)	Water Content (%)
PWSS-21	52.4	52.8	103.7	2.23	2.35	5.3
PWSS-22	52.4	52.7	103.5	2.23	2.34	4.7
PWSS-23	53	53.6	103.6	2.31	2.44	5.4
PWSS-24	54.2	52.4	103.3	2.28	2.38	4.2
PWSS-25	52.4	54.4	104.5	2.21	2.32	4.9
PWSS-26	54.6	52.7	103.8	2.19	2.31	5.4
PWSS-27	53	52.2	103.8	2.22	2.33	4.7
PWSS-28	52.5	54.2	103.5	2.26	2.38	4.8
PWSS-29	52.4	52.5	103.8	2.25	2.35	4.6
PWSS-30	54.1	52.7	104.3	2.23	2.35	5.7
PWSS-31	53.4	52.5	103.7	2.28	2.40	4.9
PWSS-32	52.5	52.9	103.6	2.25	2.36	4.6
PWSS-33	52.3	52.3	103.4	2.30	2.39	4.3
PWSS-34	51.9	53.6	103.9	2.26	2.36	4.7
PWSS-35	52.4	53.7	103.2	2.29	2.40	4.8
PWSS-36	51.9	53.2	103.5	2.29	2.40	5.3
PWSS-37	52.7	53.3	104.3	2.20	2.30	4.9
PWSS-38	52.6	52.7	103.4	2.23	2.34	5.1
PWSS-39	52.2	52.8	104.7	2.23	2.33	4.7
PWSS-40	52.4	52.5	103.4	2.25	2.36	5.1

Table A.5 Dimensions and density of PP sandstone under saturated condition.

Specimen no.	Width (mm)	Length (mm)	Height (mm)	Dry Density (g/cc)	Wet Density (g/cc)	Water Content (%)
PPSS-21	50.00	50.10	102.68	2.43	2.48	1.83
PPSS-22	52.16	52.56	101.08	2.40	2.45	2.03
PPSS-23	51.08	51.18	101.58	2.43	2.48	1.95
PPSS-24	50.40	52.88	101.38	2.46	2.52	2.36
PPSS-25	51.76	54.02	101.00	2.33	2.38	2.36
PPSS-26	51.38	53.02	100.60	2.42	2.47	2.39
PPSS-27	50.30	54.02	101.18	2.42	2.49	2.87
PPSS-28	50.30	51.00	101.66	2.42	2.65	2.51
PPSS-29	51.68	54.62	101.28	2.40	2.44	1.47
PPSS-30	51.28	52.00	101.70	2.43	2.59	2.12
PPSS-31	50.70	51.30	102.54	2.62	2.66	1.46
PPSS-32	50.20	50.50	101.26	2.44	2.78	1.93
PPSS-33	50.50	51.70	102.56	2.32	2.69	1.83
PPSS-34	50.80	51.08	101.10	2.36	2.77	1.72
PPSS-35	50.00	51.70	100.50	2.41	2.82	1.75
PPSS-36	51.60	51.70	100.60	2.34	2.75	1.77
PPSS-37	50.82	51.80	101.70	2.32	2.78	2.01
PPSS-38	51.08	51.28	101.36	2.45	2.83	2.12
PPSS-39	50.02	55.72	102.00	2.36	2.66	2.23
PPSS-40	49.74	50.60	101.48	2.43	2.99	2.28

Table A.6 Dimensions and density of PK sandstone under saturated condition.

Specimen no.	Width (mm)	Length (mm)	Height (mm)	Dry Density (g/cc)	Wet Density (g/cc)	Water Content (%)
PKSS-21	53.02	51.90	102.18	2.53	2.57	1.38
PKSS-22	53.16	51.98	102.10	2.54	2.58	1.53
PKSS-23	51.57	53.80	101.71	2.54	2.59	1.84
PKSS-24	51.56	53.90	101.48	2.54	2.57	1.20
PKSS-25	51.50	53.64	101.96	2.54	2.58	1.52
PKSS-26	51.46	53.96	101.81	2.54	2.58	1.62
PKSS-27	51.77	53.91	101.98	2.54	2.58	1.63
PKSS-28	51.44	54.06	101.90	2.52	2.56	1.63
PKSS-29	51.92	52.24	101.88	2.55	2.61	1.83
PKSS-30	51.68	54.00	101.68	2.52	2.57	1.68
PKSS-31	51.38	53.86	101.80	2.52	2.57	1.68
PKSS-32	50.94	50.92	101.60	2.60	2.63	1.14
PKSS-33	50.08	51.40	101.00	2.64	2.67	1.26
PKSS-34	51.82	51.28	102.86	2.47	2.52	1.93
PKSS-35	51.14	52.00	102.50	2.50	2.54	1.58
PKSS-36	52.50	50.38	104.10	2.47	2.51	1.90
PKSS-37	51.00	52.00	101.38	2.53	2.56	1.21
PKSS-38	51.28	52.88	101.72	2.48	2.51	1.01
PKSS-39	51.12	51.88	102.50	2.52	2.55	1.08
PKSS-40	51.00	51.58	104.40	2.47	2.52	1.88

BIOGRAPHY

Mr. Ronnachai Dasri was born on February 4, 1988 in Surin province, Thailand. He received his Bachelor's Degree in Engineering (Geotechnology) from Suranaree University of Technology in 2010. For his post-graduate, he continued to study with a Master's degree in the Geological Engineering Program, Institute of Engineering, Suranaree university of Technology. During graduation, 2010-2012, he was a part time worker in position of research assistant at the Geomechanics Research Unit, Institute of Engineering, Suranaree University of Technology.

